FINITE ELEMENT LARGE AMPLITUDE FREE FLEXURAL VIBRATION ANALYSIS OF ISOTROPIC PLATES

A THESIS SUBMITTED IN PARTIAL FULFILMENT
OF THE REQUIREMENTS FOR THE DEGREE OF

Master of Technology
in
Civil Engineering

By

ASIM KUMAR MISHRA

DEPARTMENT OF CIVIL ENGINEERING
NATIONAL INSTITUTE OF TECHNOLOGY
ROURKELA-769008,
2008

FINITE ELEMENT LARGE AMPLITUDE FREE FLEXURAL VIBRATION ANALYSIS OF ISOTROPIC PLATES

A THESIS SUBMITTED IN PARTIAL FULFILMENT
OF THE REQUIREMENTS FOR THE DEGREE OF

Master of Technology
in
Civil Engineering

By
ASIM KUMAR MISHRA

Under the guidance of
Prof. M. R. Barik

DEPARTMENT OF CIVIL ENGINEERING
NATIONAL INSTITUTE OF TECHNOLOGY
ROURKELA-769008,
2008

NATIONAL INSTITUTE OF TECHNOLOGY
ROURKELA – 769008, ORISSA
INDIA

CERTIFICATE

This is to certify that the thesis entitled, **"FINITE ELEMENT LARGE AMPLITUDE FREE FLEXURAL VIBRATION ANALYSIS OF ISOTROPIC PLATES"** submitted by **Mr. Asim Kumar Mishra** in partial fulfillment of the requirements for the award of **Master of Technology** Degree in **Civil Engineering** with specialization in **Structural Engineering** at the National Institute of Technology, Rourkela (Deemed University) is an authentic work carried out by him under my supervision and guidance.

To the best of my knowledge, the matter embodied in this thesis has not been submitted to any other University/ Institute for the award of any degree or diploma.

Dr. M. R. Barik
Dept of Civil Engineering
National Institute of Technology
Rourkela – 769008

Date: 30th May 2008
Place: Rourkela

ACKNOWLEDGEMENT

I wish to express my sincere gratitude to **Prof. M. R. Barik,** for his excellent guidance and perennial encouragement and support during the course of my work in the last one year. I truly appreciate and value his profound knowledge, esteemed supervision and encouragement from the beginning to the end of this thesis.

My special thanks are due to **Prof K. C. Patra,** Head of the Civil Engineering Department, for all the facilities provided to successfully complete this work.

I am also very thankful to all the faculty members of the department, especially Structural Engineering specialization for their constant encouragement during the project.

I also take the opportunity to thank all my friends who have directly or indirectly helped me in my project work and in the completion of this report.

Last but not the least I would like to thank my parents, who taught me the value of hard work by their own example. I would like to share this bite of happiness with my father, mother and brother Amit. They rendered me enormous support during the whole tenure of my stay at NIT, Rourkela.

Date: 30th May 2008

Asim Kumar Mishra
20601021
NIT, Rourkela

CONTENTS

ABSTRACT

Structural components are generally subjected to dynamic loadings in their working life. Very often these components may have to perform in severe dynamic environment wherein the maximum damage results from the resonant vibration.

Susceptibility to fracture of materials due to vibration is determined from stress and frequency. Maximum amplitude of the vibration must be in the limited for the safety of the structure. Hence vibration analysis has become very important in designing a structure to know in advance its response and to take necessary steps to control the structural vibrations and its amplitudes.

The non-linear or large amplitude flexural vibration of plates has received considerable attention in recent years because of the great importance and interest attached to the structures of low flexural rigidity. These easily deformable structures vibrate at large amplitudes. The solution obtained based on the lineage models provide no more than a first approximation to the actual solutions. The increasing demand for more realistic models to predict the responses of elastic bodies combined with the availability of super computational facilities have enabled researchers to abandon the linear theories in favor of non-linear methods of solutions.

In the present investigation, large amplitude vibration of several rectangular and skew plates has been studied using an isoparametric quadratic plate bending element for the finite element method. The formulations have incorporated the shear deformation of the plates. Plates with various boundary conditions have been considered in the study. The effect of variations in the Poisson’s ratio, thickness parameter & plate aspect ratio on the non-linear frequency ratio has also been included in the research.

NOMENCLATURE

A	Amplitude of vibration
a, b	Plate dimensions
$[B]$	Strain matrix
$[B_L]$	Stain matrix associated with linear strain components
$[B_{NL}]$	Strain matrix associated with non-linear strain components
C	Particular displacement to be normalized to desired amplitude
$[D]$	Rigidity matrix
E	Young's modulus of elasticity
G	Shear modulus
h	Plate thickness
$[J]$	Jacobian matrix
$[K]$	Stiffness matrix
$[K_L]$	Linear stiffness matrix
$[K_{NL}]$	Non-linear stiffness matrix
$[K_S]$	Secant stiffness matrix
$[M]$	Mass matrix
$[N]$	Shape functions
$[N_1], [N_2]$	First and second degree stiffness matrix
N_x , N_y	Normal forces per unit length
N_{xy}	Twisting moment per unit length
M_x , M_y	Bending moment per unit length
M_{xy}	Twisting moment per unit length
$\{R\}$	Vector of generalized forces
S_X , S_Y	Shear rigidities
U , V , W	Displacements at any point
u , v , w	Middle surface displacements
x , y , z	Cartesian coordinate system
α	Non-uniform shear strain factor

$\{\delta\}$	Vector of nodal displacements
$\{\delta_r\}$	Displacements at r^{th} node
$\{\varepsilon\}$	Strain vector
$\{\varepsilon_L\}, \{\varepsilon_{NL}\}$	Vectors of linear and non-linear strain components
θ_x , θ_y	Rotations of mid-surface normals
λ	Eigenvalue
υ	Poisson's ratio
ρ	Mass density
$\{\sigma\}$	Vector of stress resultants
$\{\sigma_L\}, \{\sigma_{NL}\}$	Vectors of linear and non-linear components of stress resultants
ϕ_x , ϕ_y	Shear rotations of mid-surface normals
$\{\phi\}$	Modal vector
ϖ_L , ϖ_{NL}	Linear and non-linear frequency
ξ , η	Natural coordinates

LIST OF FIGURES

LIST OF TABLES

Chapter - 1

INTRODUCTION

INTRODUCTION

1.1 GENERAL

Structural components are generally subjected to dynamic loadings in their working life. Very often these components may have to perform in severe dynamic environment wherein the maximum damage results from the resonant vibration. In the vehicles used in transport such as ships and aircrafts, vibration results in discomfort to the crew and passengers. Human reaction to vibration in the range of 4Hz to 16Hz is more sensitive because natural frequencies of the body can be excited and may cause serious physiological effects.

Susceptibility to fracture of materials due to vibration is determined from stress and frequency. Maximum amplitude of the vibration must be in the limited for the safety of the structure. Hence vibration analysis has become very important in designing a structure to know in advance its response and to take necessary steps to control the structural vibrations and its amplitudes.

For a long time, the problems in structural mechanics have been solved using linear or linearized equations representing structural behavior, which is far from actual. The high strength of some materials such as composites results in the requirement of low thicknesses of laminates in structures which are often subjected to severe dynamic environments. Thus, these structures may vibrate with large amplitudes, where linear vibration analysis becomes insufficient. Also because of the anisotropic properties of these materials the analysis of composite structures becomes a complex task compared with the conventional material structures. The availability of superior computational facilities has now enabled researchers to abandon the long adopted linear theories in favor of non-linear methods of solutions.

In general, non-linearity in structural mechanics can arise in many ways. The generalized Hooke’s law is not valid if material stress-strain behavior is non-linear. This type of non-linearity is generally known as the material or physical non-linearity. Alternatively, a different type of non-linearity based on the deformations of an elastic body is possible in many instances. Problems involving deformations that are large are called geometrically non-linear problems. Deformation of an elastic body can also be of a magnitude that does not

overstrain the material or produce stretching under large deformations and thus lead to curvature-displacement non-linearity. Since this is deformation dependent it is also classified as a geometric non-linearity. Combinations of geometric and physical type of non-linearity are also possible. If during loading a displacement boundary condition changes, e.g., a degree of freedom which was free becomes restrained at a certain load level, the response is linear only prior to the change of boundary condition. It is well known that static and dynamic responses of bodies governed by non-linearity complicate the analytical investigations. This is mainly due to the fact that the advantages of uniqueness and superposition of solutions, characteristic of problems governed by the linear differential equations, do not exist in problems governed by non-linear differential equations.

The solution of non-linear problems by the finite element method is usually attempted by one of the three basic techniques: incremental or stepwise procedures, iterative or Newton methods and step-iterative or mixed procedures. In case of incremental procedures, load is subdivided into many small partial loads or increments usually equal in magnitude though generally they need not be equal. The load is applied one increment at a time, and during the application of each increment the equations are assumed to be linear. In other words a fixed value of stiffness matrix is assumed throughout each increment, but stiffness matrix may take different values during different load increments. The solution for each step of loading is obtained as an increment of the displacements. These displacement increments are accumulated to give the total displacement at any stage of loading and the incremental process is repeated until the total load is reached. The incremental method is analogous to the numerical method used for the integration of systems of linear or non-linear differential equations, such as the Euler method or Runge-Kutta method.

The iterative procedure is a sequence of calculations in which the body or structure is fully loaded in each iteration. Because some approximate constant value of the stiffness matrix is used in each step, equilibrium is not necessarily satisfied. After each iteration, the portion of the total loading that is not balanced is calculated and used in the next step to compute an additional increment of displacements. The process is repeated until equilibrium is approximated to some acceptable degree. Some of the iterative methods are direct iteration technique and Newton-Raphson techniques. The mixed procedures utilize a combination of the incremental and iterative schemes. Here the load is applied incrementally, but after each increment successive iterations are performed.

1.2 PRESENT INVESTIGATION

In the current investigation the main objective is to find out the non-linear frequency ratios of free un-damped vibration of plates. Finite element method has been adopted for the current analysis. An isoparametric quadratic plate bending element has been used. It also considers the shear deformation of the plate. Hence the formulation is applicable to both thin as well as thick plates. Consistent mass matrix has been used.

As the higher order terms in the strain-displacement relations are not known, in order to obtain the solution for non-linear free vibration problem an iterative procedure is adopted using linear strain-displacement relations for the first iteration. For the successive iterations the higher order terms of the strain-displacement relations have been evaluated from the scaled eigenvectors corresponding to a given amplitude at a prescribed point of the previous iterations. The iteration process is continued until required convergence is reached.

In the present investigation, non-linear free vibration analysis is done for several quadrangular plates. Various boundary conditions have been considered. The effect of variations in the some material and/or geometric properties of the plate have also been studied.

Chapter - 2

LITERATURE REVIEW

LITERATURE REVIEW

The large amplitude vibration of plates and shells has received considerable attention in recent years because of great importance and interest attached to the structures of low flexural rigidity. As a result of which large amplitude vibrations of plates of various geometries have received much attention [18, 19, 20].

In the area of non-linear vibration of plates of various shapes, rectangular plates have been studied more frequently than others. Most of the work is based on the governing equations in terms of stress function and lateral displacement. The governing non-linear equations of motion can be suitably modified to include the effects of several complicating factors such as transverse shear, in-plane forces and the like.

Large amplitude flexural vibration of thin rectangular plates is studied by Rao et al. [13] using a direct finite element formulation. The formulation is based on an appropriate linearization of strain displacement relation and an iterative method of solution has been used. They have observed the period ratios for the square as well as rectangular plates under different boundary conditions.

The geometrically non-linear free vibrations of thin isotropic and laminated rectangular composite plates with fully clamped edges have been successfully investigated by Bikri et al. [3] using a theoretical model based on Hamilton's principle and spectral analysis. The work has been further extended [2] to the plates with other boundary conditions in order to determine their fundamental non-linear mode shape and associated amplitude-dependent resonant frequencies and flexural stress distribution.

Sarma et al. [17] have formulated the non-linear vibration of a rectangular plate by using Kirchhoff's hypothesis and von Karman type strain-displacement relations. In-plane deformations are included and the corresponding inertia terms are neglected in this formulation. The restoring force function in the equation of motion is found to be a cubic polynomial, which is of Duffing type or a combination of quadratic and cubic terms. The exact solution of the equation of motion is presented in an expression which is evaluated numerically for obtaining the frequency corresponding to the specified maximum amplitude.

Rao et al. [14] have studied the large amplitude vibration of rectangular plates with and without stiffeners. They have taken the shear deformation of the plate and the stiffeners into due consideration in their formulation. Also the formulation considers the in-plane inertia of the plate.

Large amplitude flexural vibrations of clamped as well as simply supported isotropic elastic rhombic plates were investigated by Ray et al.[15], the effects of shear deformation and rotary inertia being included. The governing equations for plates of transversely isotropic material were solved by the well-known Galerkin procedure. A number of cases were solved for different edge conditions of the rhombic plates, indicating the significant influences of skew angle, transverse shear deformation and rotary inertia.

Large amplitude free flexural vibration analysis of composite stiffened plates have been carried out by Goswami & Kant [7] using a C^0 nine-noded Lagrangian element. The element is based on the first order shear deformation theory. The large deformation effect of the stiffened plated structures has been taken care by the dynamic version of von Karman's field equations. The non-linear equations obtained have been solved by the direct iteration technique using the linear modeshapes as the starting vectors.

Harras et al. [8] have made an extensive study on symmetrically laminated rectangular CFRP plates. They have formulated the geometrically non-linear behavior and analyzed for fully clamped support condition. In their study they have reported the frequency amplitude dependence. The non-linear solutions have been performed by using the basic plate functions.

Non-linear free vibration analysis is carried out by Saha et al. [16] on square plates with different boundary conditions. They have focused only on geometric non-linearity and proposed a new methodology that can be employed for plate structure problems having any combination of boundary conditions to determine the non-linear frequencies and mode shapes. The large amplitude vibration problem is analyzed in two parts. The static problem corresponding to a uniform transverse loading is solved first and the dynamic problem is subsequently taken up with the known deflection field. Both these problems are formulated

through energy method, the underlying principle being the extremisation of total energy of the system in its equilibrium state. The solution methodology employs an iterative numerical scheme using the technique of successive relaxation.

A nine-noded isoparametric plate-bending element has been used by Pandit et al. [12] for the analysis of free un-damped vibration of isotropic and fiber reinforced laminated composite plates. The effect of shear deformation is incorporated in the formulation by considering the first-order shear deformation theory for the analysis. An effective mass lumping scheme with rotary inertia has been recommended. Two types of mass lumping schemes have been formed. In one lumping scheme rotary inertia has also been introduced.

Large-amplitude free vibration analysis of simply supported thin isotropic skew plates has been presented by Das et al. [5]. In this paper the large deformation has been imparted statically by subjecting the plate under uniform transverse pressure. The mathematical formulation is based on the variational principle in which the displacement fields are assumed as a combination of orthogonal polynomial or transcendental functions, each satisfying the corresponding boundary conditions of the plate. The large-amplitude dynamic problem has been addressed by solving the corresponding static problem first, and subsequently with the resultant displacement field, the problem is formulated. The vibration frequencies are obtained from the solution of a standard eigenvalue problem. Entire computational work has been carried out in a normalized square domain obtained through an appropriate domain mapping technique.

Chapter - 3

THEORY & FINITE ELEMENT FORMULATION

THEORY AND FINITE ELEMENT FORMULATION

3.1 FINITE ELEMENT FORMULATION

In the finite element analysis, the continuum is divided into a finite number of elements having finite dimensions and reducing the continuum having infinite degrees of freedom to finite number of unknowns. The formulation presented here is based on assumed displacement pattern within the element and can be applied to linear, quadratic, cubic or any other higher order element by incorporating appropriate shape functions.

In the following the element mass and stiffness matrices of the plate are derived. The element mass and stiffness matrices are then assembled to form the overall mass and stiffness matrices. Necessary boundary conditions are then incorporated. Reduced integration technique has been used to obtain the element mass and stiffness matrices.

An isoparametric quadratic plate bending element (Fig. 3.1) is chosen in the present analysis.

3.2 ASSUMPTIONS

The formulation is based on the following assumptions:

(i) The material of the plate obeys Hooke's law.

(ii) The bending deformations follow Mindlin's hypothesis therefore the normal perpendicular to the middle plane of the plate before bending remains straight, but not necessarily normal to the middle plane of the plate after bending.

(iii) The deflection in the z-direction is a function of x and y only.

(iv) The transverse normal stresses are neglected

3.3 EQUILIBRIUM EQUATIONS

The equations of motion for free un-damped vibration of an elastic system undergoing large displacements can be expressed in the following matrix form,

$$[K]\{\delta\} + [M]\{\ddot{\delta}\} = \{0\} \tag{3.3.1}$$

in which $[K]$ and $[M]$ are overall stiffness and mass matrices and $\{\delta\}$ is the displacement vector.

3.4 SHAPE FUNCTIONS

If displacements at a node r of a quadratic isoparametric element are u_r, v_r, w_r, θ_{xr} and θ_{yr}, then at any point inside the element

$$\begin{Bmatrix} x \\ y \end{Bmatrix} = \sum_{r=1}^{8} N_r [I_2] \begin{Bmatrix} x_r \\ y_r \end{Bmatrix} \tag{3.4.1}$$

and

$$\{\delta\} = \sum_{r=1}^{8} N_r [I_5] \{\delta_r\} \tag{3.4.2}$$

in which, N_r is the shape function at a node r

$$\{\delta\}^T = \begin{Bmatrix} u & v & w & \theta_x & \theta_y \end{Bmatrix} \tag{3.4.3}$$

$$\{\delta_r\}^T = \begin{Bmatrix} u_r & v_r & w_r & \theta_{xr} & \theta_{yr} \end{Bmatrix} \tag{3.4.4}$$

The shape functions are expressed in terms of non-dimensional parameters ξ and η. The Jacobian matrix $[J]$ and its inverse required for all the later calculations are given by

$$[J] = \begin{bmatrix} \frac{\partial x}{\partial \xi} & \frac{\partial y}{\partial \xi} \\ \frac{\partial x}{\partial \eta} & \frac{\partial y}{\partial \eta} \end{bmatrix} \qquad [J]^{-1} = \begin{bmatrix} \frac{\partial \xi}{\partial x} & \frac{\partial \mu}{\partial y} \\ \frac{\partial \xi}{\partial x} & \frac{\partial \eta}{\partial y} \end{bmatrix} \tag{3.4.5}$$

3.5 PLATE ELEMENT FORMULATION

The displacement field at any point within the element is given by

$$\{f\} = \begin{Bmatrix} U \\ V \\ W \end{Bmatrix} = \begin{Bmatrix} u - z\theta_x \\ v - z\theta_y \\ w \end{Bmatrix} \tag{3.5.1}$$

Owing to the shear deformations, certain warping in the section occurs as shown in Fig. 3.2. However, considering the rotations θ_x and θ_y as the average and linear variation

Fig. 3.1 QUADRATIC ISOPARAMETRIC PLATE ELEMENT

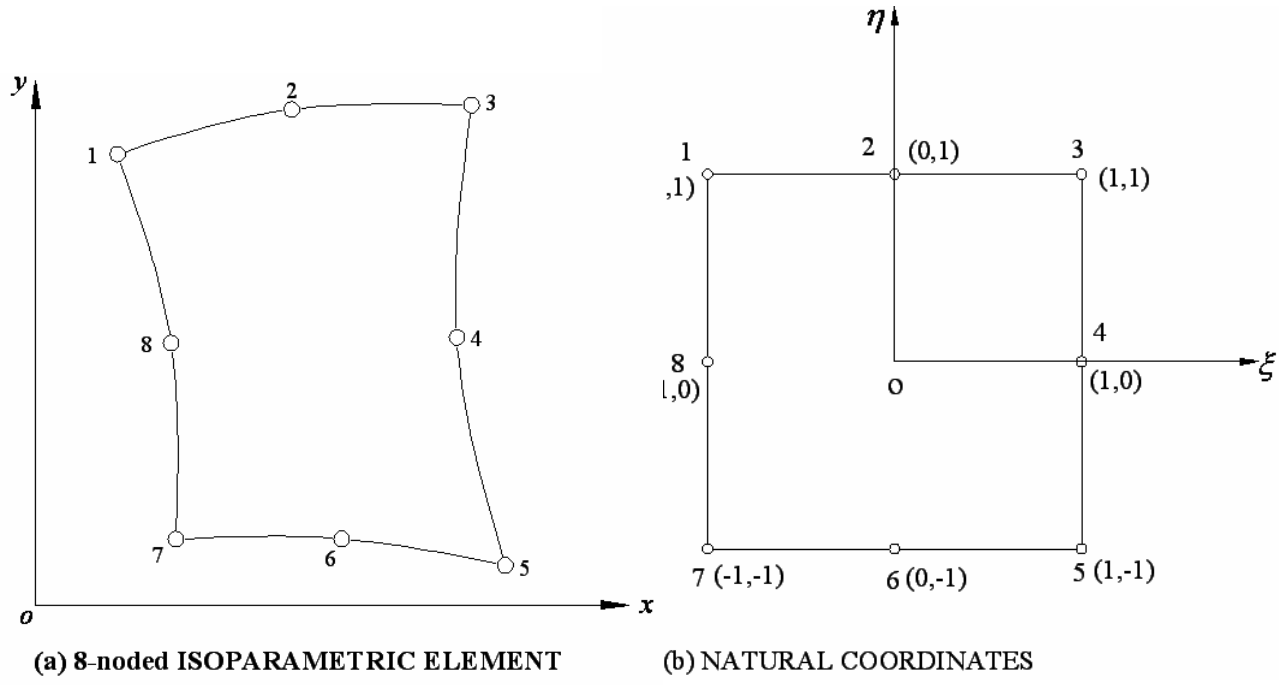

(a) 8-noded ISOPARAMETRIC ELEMENT (b) NATURAL COORDINATES

Fig. 3.2 DEFORMATION OF PLATE CROSS-SECTION

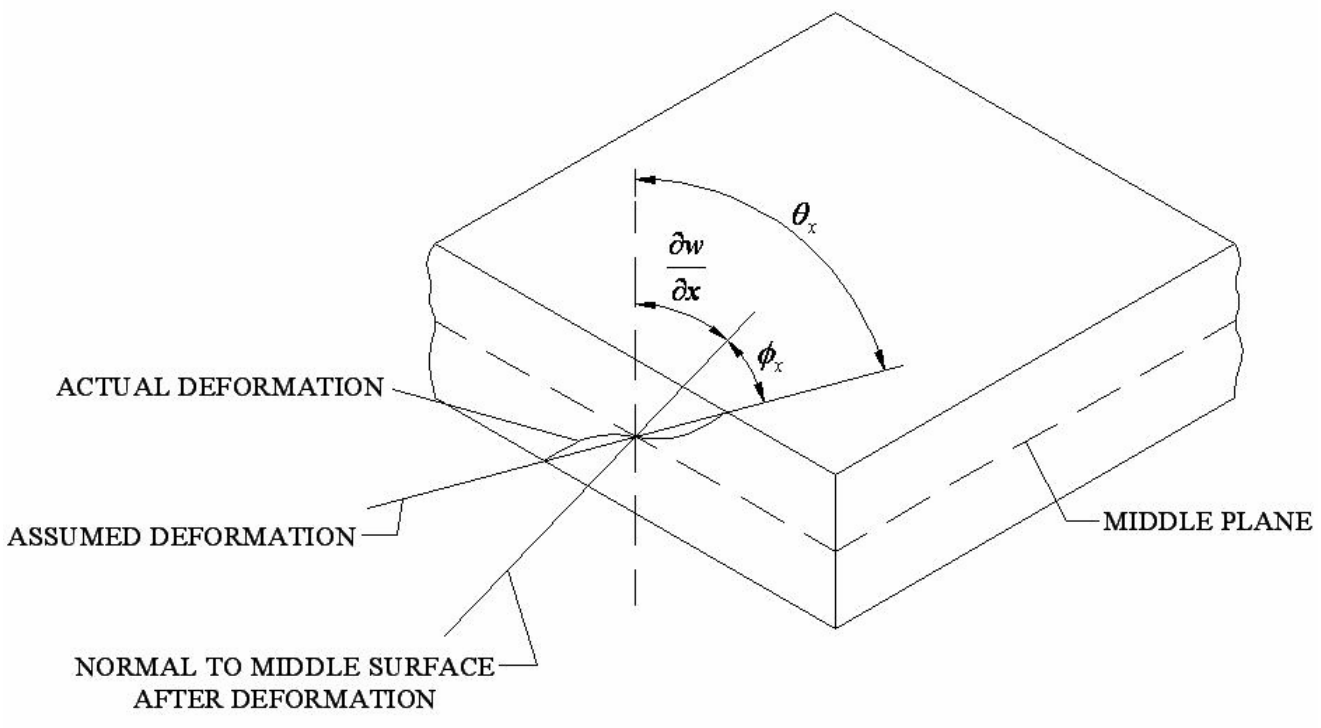

along the thickness of the plate, the angles ϕ_x and ϕ_y denoting the average shear deformation in x and y directions respectively are given by

$$\begin{Bmatrix} \theta_x \\ \theta_y \end{Bmatrix} = \begin{Bmatrix} \frac{\partial w}{\partial x} + \phi_x \\ \frac{\partial w}{\partial y} + \phi_y \end{Bmatrix} \tag{3.5.2}$$

3.5.1 Linear and Non-Linear Stiffness Matrices

The plate strains are described in terms of middle surface displacements *i. e.* $x-y$ plane coincides with the middle surface as shown in Fig.3.3 (a). The strain matrix is given by

$$\{\varepsilon\} = \begin{Bmatrix} \varepsilon_x \\ \varepsilon_y \\ \gamma_{xy} \\ -\frac{\partial^2 w}{\partial x^2} \\ -\frac{\partial^2 w}{\partial y^2} \\ 2\frac{\partial^2 w}{\partial x \partial y} \\ -\phi_x \\ -\phi_y \end{Bmatrix} \tag{3.5.3}$$

The stress matrix is given by

$$\{\sigma\} = \begin{Bmatrix} N_x \\ N_y \\ N_{xy} \\ M_x \\ M_y \\ M_{xy} \\ V_x \\ V_y \end{Bmatrix} \tag{3.5.4}$$

The stresses are defined in terms of usual stress resultants: $N_x = \sigma_x h$, where σ_x is the average membrane stress etc. Now if the deformed shape is considered as shown in the

Fig. 3.3 (a) In-plane and bending resultants for a flat plate
(b) Increase of middle surface length due to lateral displacement

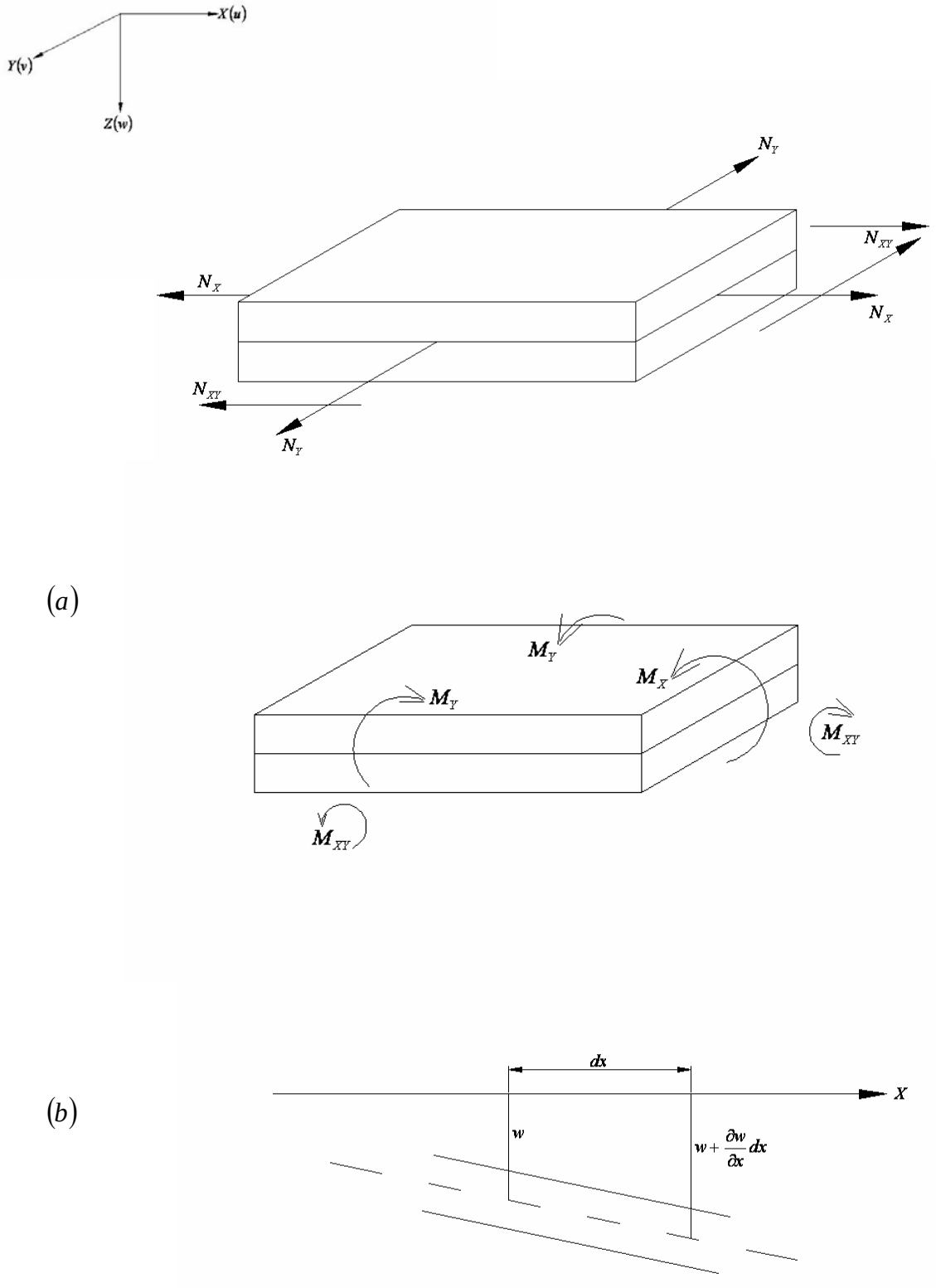

Fig. 3.3(b) it is seen that displacement w produces some additional extension in the x and y directions of the middle surface and the length dx stretches to

$$dx' = dx\sqrt{1+(\partial w/\partial x)^2} = dx\left\{1+\frac{1}{2}(\partial w/\partial x)^2 + ...\right\} \tag{3.5.5}$$

In defining the x- elongation the following relationship can be written (to second approximation)

$$\varepsilon_x = (\partial u/\partial x) + \frac{1}{2}(\partial w/\partial x)^2 \tag{3.5.6}$$

In the similar manner considering the other components the strain is given by

$$\{\varepsilon\} = \{\varepsilon_L\} + \{\varepsilon_{NL}\} \tag{3.5.7}$$

where

$$\{\varepsilon_L\} = \begin{Bmatrix} \dfrac{\partial u}{\partial x} \\ \dfrac{\partial v}{\partial y} \\ \left(\dfrac{\partial u}{\partial y} + \dfrac{\partial v}{\partial x}\right) \\ -\dfrac{\partial^2 w}{\partial x^2} \\ -\dfrac{\partial^2 w}{\partial y^2} \\ 2\dfrac{\partial^2 w}{\partial x \partial y} \\ -\phi_x \\ -\phi_y \end{Bmatrix} \quad \text{and} \quad \{\varepsilon_{NL}\} = \begin{Bmatrix} \dfrac{1}{2}\left(\dfrac{\partial w}{\partial x}\right)^2 \\ \dfrac{1}{2}\left(\dfrac{\partial w}{\partial y}\right)^2 \\ \left(\dfrac{\partial w}{\partial x}\right)\left(\dfrac{\partial w}{\partial y}\right) \\ 0 \\ 0 \\ 0 \\ 0 \\ 0 \end{Bmatrix} \tag{3.5.8}$$

in which the first term is the linear expression and the second term gives non-linear terms. If linear elastic behavior is considered, the stress-strain relationship is written as

$$\{\sigma\} = [D]\{\varepsilon\} = [D](\{\varepsilon_L\} + \{\varepsilon_{NL}\}) = \{\sigma_L\} + \{\sigma_{NL}\} \tag{3.5.9}$$

where $[D]$, the rigidity matrix is given by

$$[D]=\begin{bmatrix} DXA & DIA & 0 & 0 & 0 & 0 & 0 & 0 \\ DIA & DYA & 0 & 0 & 0 & 0 & 0 & 0 \\ 0 & 0 & DXYA & 0 & 0 & 0 & 0 & 0 \\ 0 & 0 & 0 & DXF & DIF & 0 & 0 & 0 \\ 0 & 0 & 0 & DIF & DYF & 0 & 0 & 0 \\ 0 & 0 & 0 & 0 & 0 & DXYF & 0 & 0 \\ 0 & 0 & 0 & 0 & 0 & 0 & S_x & 0 \\ 0 & 0 & 0 & 0 & 0 & 0 & 0 & S_y \end{bmatrix} \qquad (3.5.10)$$

in which

$$DXA=\frac{Eh}{\left(1-\upsilon^2\right)} \qquad DIA=\upsilon\times DXA \qquad DYA=DXA \qquad DXYA=\left(\frac{1-\upsilon}{2}\right)\times DXA$$

$$DXF=\frac{Eh^3}{12\times\left(1-\upsilon^2\right)} \qquad DIF=\upsilon\times DXF \qquad DYF=DXF \qquad DXYF=\left(\frac{1-\upsilon}{2}\right)\times DXF$$

$$S_X=S_Y=\alpha\times Gh$$

where

$E = Modulus\ of\ \ Elasticity$

$G = Shear\ \ Modulus$

$\upsilon = Poisson's\ \ Ratio$

$h = Thickness\ of\ \ the\ \ plate$

and

α is a factor to account for the non-uniformity of the shear strain distribution. it is taken as $\left(5/6\right)$ for isotropic materials.

The non-linear strain components of equation (3.5.8) can be conveniently written as

$$\{\varepsilon_{NL}\}=\frac{1}{2}\begin{bmatrix} \frac{\partial w}{\partial x} & 0 \\ 0 & \frac{\partial w}{\partial y} \\ \frac{\partial w}{\partial y} & \frac{\partial w}{\partial x} \\ 0 & 0 \\ 0 & 0 \\ 0 & 0 \\ 0 & 0 \\ 0 & 0 \end{bmatrix}\begin{Bmatrix} \frac{\partial w}{\partial x} \\ \frac{\partial w}{\partial y} \end{Bmatrix}=\frac{1}{2}[A]\{\theta\} \qquad (3.5.11)$$

The slopes can be related to nodal parameters as follows

$$\{\theta\} = \begin{Bmatrix} \frac{\partial w}{\partial x} \\ \frac{\partial w}{\partial y} \end{Bmatrix} = \sum_{i=1}^{8} \begin{bmatrix} 0 & 0 & \frac{\partial N_i}{\partial x} & 0 & 0 \\ 0 & 0 & \frac{\partial N_i}{\partial y} & 0 & 0 \end{bmatrix} \begin{Bmatrix} u_i \\ v_i \\ w_i \\ \theta_{xi} \\ \theta_{yi} \end{Bmatrix} = [G]\{\delta\} \tag{3.5.12}$$

in which

$$[G] = \sum_{i=1}^{8} \begin{bmatrix} 0 & 0 & \frac{\partial N_i}{\partial x} & 0 & 0 \\ 0 & 0 & \frac{\partial N_i}{\partial y} & 0 & 0 \end{bmatrix} \tag{3.5.13}$$

Taking variation of equation (3.5.11)

$$d\{\varepsilon_{NL}\} = \frac{1}{2} d[A]\{\theta\} + \frac{1}{2}[A]\, d\{\theta\} = [A]\{G\}\, d\{\delta\} \tag{3.5.14}$$

The manipulation of equation (3.5.14) is due to an interesting property of the matrices $[A]$ and $\{\theta\}$. $\{\varepsilon\}$ is approximated as

$$d\{\varepsilon\} = \left[\bar{B}\right] d\{\varepsilon\} \tag{3.5.15}$$

where

$$\left[\bar{B}\right] = [B_L] + [B_{NL}(\delta)] \tag{3.5.16}$$

in which $[B_L]$, is the same matrix as in linear infinitesimal strain analysis and is given by

$$[B_L] = \sum_{i=1}^{8} \begin{bmatrix} \frac{\partial N_i}{\partial x} & 0 & 0 & 0 & 0 \\ 0 & \frac{\partial N_i}{\partial y} & 0 & 0 & 0 \\ \frac{\partial N_i}{\partial y} & \frac{\partial N_i}{\partial x} & 0 & 0 & 0 \\ 0 & 0 & 0 & -\frac{\partial N_i}{\partial x} & 0 \\ 0 & 0 & 0 & 0 & -\frac{\partial N_i}{\partial y} \\ 0 & 0 & 0 & \frac{\partial N_i}{\partial y} & \frac{\partial N_i}{\partial x} \\ 0 & 0 & \frac{\partial N_i}{\partial x} & -N_i & 0 \\ 0 & 0 & \frac{\partial N_i}{\partial y} & 0 & -N_i \end{bmatrix} \tag{3.5.17}$$

Only $[B_{NL}]$ depends on the displacements. In general, $[B_{NL}]$ is found to be a linear function of such displacements. Therefore,

$$d\{\varepsilon\} = d\{\varepsilon_L\} + d\{\varepsilon_{NL}\} = \left([B_L] + [B_{NL}]\right) d\{\delta\} \tag{3.5.18}$$

Comparing equations (3.5.12), (3.5.14) and (3.5.18) it is found that

$$[B_{NL}] = [A]\{G\} \tag{3.5.19}$$

and

$$\{\varepsilon_{NL}\} = \frac{1}{2}[B_{NL}]\{\delta\} \tag{3.5.20}$$

The virtual work equation in Lagrangian coordinate system is

$$\int_V d\{\varepsilon\}^T \{\sigma\}\, dv - d\{\sigma\}^T \{R\} = \{0\} \tag{3.5.21}$$

where $d\{\varepsilon\}$ is the variation in the Green's strain vector $\{\varepsilon\}$, associated with the displacements $d\{\delta\}$. $\{\sigma\}$ is the Poila-Kirchoff's stress and $\{R\}$ is a vector of generalized forces associated with the displacements $d\{\delta\}$.

The finite element approximation to the equation (3.5.21) in the B-notation is

$$d\{\delta\}^T \int_V \left[\bar{B}\right]^T \{\sigma\}\, dv - d\{\sigma\}^T \{R\} = \{0\} \tag{3.5.22}$$

which, because $d\{\delta\}$ is arbitrary, gives the equilibrium equation as

$$\int_V \left[\bar{B}\right]^T [D]\{\varepsilon\}\, dv - \{R\} = \{0\} \tag{3.5.23}$$

or $$\int_V ([B_L] + [B_{NL}])^T [D]\left([B_L] + \frac{1}{2}[B_{NL}]\right)\{\delta\}\, dv - \{R\} = \{0\}$$

or $$[K_S]\{\delta\} - \{R\} = \{0\} \tag{3.5.24}$$

where $[K_S]$ =

$$\int_V \left([B_L]^T [D][B_L] + [B_{NL}]^T [D][B_L] + \frac{1}{2}[B_L]^T [D][B_{NL}] + \frac{1}{2}[B_{NL}]^T [D][B_{NL}]\right) dv \tag{3.5.25}$$

If N-notation is followed, the matrix $[K_S]$ would be obtained as

$$[K_S] = \left\{[K_0] + \frac{1}{2}[N_1] + \frac{1}{2}[N_2]\right\} \tag{3.5.26}$$

The first term in the curly brackets of the above equation *i. e.* $[K_0]$ is independent of the displacements $\{\delta\}$. $[N_1]$ is linearly dependent upon $\{\delta\}$ and $[N_2]$ is quadratically dependent upon $\{\delta\}$. The matrix $[K_S]$ is known as secant stiffness matrix. The secant stiffness matrix obtained with B-notation is un-symmetric and that obtained with N-notation is symmetric. The correlation between the two notations is expressed as

$$[K_0] = \int_V [B_L]^T [D][B_L]\, dv \tag{3.5.27}$$

$$[N_1] = \int_V \left([B_L]^T [D][B_{NL}] + [B_{NL}]^T [D][B_L] + [G]^T [S_L][G]\right) dv \tag{3.5.28}$$

$$[N_2] = \int_V \left([B_{NL}]^T [D][B_{NL}] + [G]^T [S_{NL}][G]\right) dv \tag{3.5.29}$$

The matrices $[S_L]$ and $[S_{NL}]$ together give symmetric stress matrix. The symmetric stress matrix is introduced as

$$[S] = [S_L] + [S_{NL}] \tag{3.5.30}$$

where

$$[S] = \begin{bmatrix} N_x & N_{xy} \\ N_{xy} & N_y \end{bmatrix} \tag{3.5.31}$$

$$[S_L] = \begin{bmatrix} DXA\left(\frac{\partial u}{\partial x}\right) & DXYA\left(\frac{\partial u}{\partial y} + \frac{\partial v}{\partial x}\right) \\ DXYA\left(\frac{\partial u}{\partial y} + \frac{\partial v}{\partial x}\right) & DYA\left(\frac{\partial v}{\partial y}\right) \end{bmatrix} \tag{3.5.32}$$

$$[S_{NL}] = \begin{bmatrix} \frac{1}{2}\left\{ DXA\left(\frac{\partial w}{\partial x}\right)^2 + DIA\left(\frac{\partial w}{\partial y}\right)^2 \right\} & DXYA\left(\frac{\partial w}{\partial x}\right)\left(\frac{\partial w}{\partial y}\right) \\ DXYA\left(\frac{\partial w}{\partial x}\right)\left(\frac{\partial w}{\partial y}\right) & \frac{1}{2}\left\{ DIA\left(\frac{\partial w}{\partial x}\right)^2 + DYA\left(\frac{\partial w}{\partial y}\right)^2 \right\} \end{bmatrix} \tag{3.5.33}$$

From the above relations, it can be deduced that

$$[K_L] = [K_0] \tag{3.5.34}$$

and non-linear stiffness matrix

$$[K_{NL}] = \frac{1}{2}[N_1] + \frac{1}{3}[N_2] \qquad \text{in N-notation}$$

$$= \int_V \left([B_{NL}]^T [D][B_L] + \frac{1}{2}[B_L]^T [D][B_{NL}] + \frac{1}{2}[B_{NL}]^T [D][B_{NL}] \right) dv$$

in B-notation (3.5.35)

3.5.2 Mass Matrix

The acceleration field at any point in the plate is given by

$$\left\{ \ddot{f} \right\} = \begin{Bmatrix} \ddot{u} - z\ddot{\theta}_x \\ \ddot{v} - z\ddot{\theta}_y \\ \ddot{w} \end{Bmatrix}$$

$$= \begin{bmatrix} 1 & 0 & 0 & -z & 0 \\ 0 & 1 & 0 & 0 & -z \\ 0 & 0 & 1 & 0 & 0 \end{bmatrix} \begin{Bmatrix} \ddot{u} \\ \ddot{v} \\ \ddot{w} \\ \ddot{\theta}_x \\ \ddot{\theta}_y \end{Bmatrix}$$

$$= [G_P] \begin{Bmatrix} \ddot{u} \\ \ddot{v} \\ \ddot{w} \\ \ddot{\theta}_x \\ \ddot{\theta}_y \end{Bmatrix} \tag{3.5.36}$$

where

$$[G_P] = \begin{bmatrix} 1 & 0 & 0 & -z & 0 \\ 0 & 1 & 0 & 0 & -z \\ 0 & 0 & 1 & 0 & 0 \end{bmatrix} \tag{3.5.37}$$

Expressing acceleration field in terms of nodal parameters

$$\left\{ \ddot{f} \right\} = [G_P][N] \left\{ \ddot{\delta} \right\}$$

in which

$$[N] = \sum_{i=1}^{8} \begin{bmatrix} N_i & 0 & 0 & 0 & 0 \\ 0 & N_i & 0 & 0 & 0 \\ 0 & 0 & N_i & 0 & 0 \\ 0 & 0 & 0 & N_i & 0 \\ 0 & 0 & 0 & 0 & N_i \end{bmatrix} \quad \text{and} \quad \left\{ \ddot{\delta} \right\} = \sum_{i=1}^{8} \begin{Bmatrix} \ddot{u}_i \\ \ddot{v}_i \\ \ddot{w}_i \\ \ddot{\theta}_{xi} \\ \ddot{\theta}_{yi} \end{Bmatrix} \tag{3.5.38}$$

Applying D' Alembert's principle for any infinitesimal element within the element, the inertia force resisting the acceleration can be written as

$$\{F_P\} = [\rho_P] \left\{ \ddot{f} \right\} dx\, dy\, dz \tag{3.5.39}$$

in which

$$[\rho_P] = \begin{bmatrix} \rho_P & 0 & 0 \\ 0 & \rho_P & 0 \\ 0 & 0 & \rho_P \end{bmatrix} \tag{3.5.40}$$

where ρ_P is the density of the plate material.

The work done by the acceleration forces for an infinitesimal element is

$$\delta W = \{f\}^T \{F_P\}$$

$$= \{\delta\}^T [N]^T [G_P]^T [\rho_P] [G_P] [N] \left\{\ddot{\delta}\right\} dx\, dy\, dz \tag{3.5.41}$$

The internal work done by the distributed acceleration forces for an entire element is

$$W = \int_V \partial W = \int_V \{\delta\}^T [N]^T [G_P]^T [\rho_P] [G_P] [N] \left\{\ddot{\delta}\right\} dx\, dy\, dz \tag{3.5.42}$$

From the above relation, the mass matrix is obtained as

$$[M] = \int_V [N]^T [G_P]^T [\rho_P] [G_P] [N]\, dx\, dy\, dz$$

or
$$[M] = \int\int [N]^T [m_P] [N]\, dx\, dy \tag{3.5.43}$$

where

$$[m_P] = \int_{-t/2}^{+t/2} [G_P]^T [\rho_P] [G_P]\, dz$$

$$= \int_{-t/2}^{+t/2} \begin{bmatrix} 1 & 0 & 0 & -z & 0 \\ 0 & 1 & 0 & 0 & -z \\ 0 & 0 & 1 & 0 & 0 \\ -z & 0 & 0 & z^2 & 0 \\ 0 & -z & 0 & 0 & z^2 \end{bmatrix} dz \tag{3.5.44}$$

After integration, $[m_P]$ is given as

$$[m_P] = \begin{bmatrix} \rho h & 0 & 0 & 0 & 0 \\ 0 & \rho h & 0 & 0 & 0 \\ 0 & 0 & \rho h & 0 & 0 \\ 0 & 0 & 0 & \dfrac{\rho h^3}{12} & 0 \\ 0 & 0 & 0 & 0 & \dfrac{\rho h^3}{12} \end{bmatrix} \tag{3.5.45}$$

The mass matrix thus obtained above is known as consistent mass matrix.

3.6 SOLUTION PROCEDURE

By assembling the finite elements and applying the kinematic boundary conditions, the equations of motion for the linear free vibration of a given plate may be written as

$$[M] \{\phi\}_0 - \lambda [K_L] \{\phi\}_0 = \{0\}$$

or $$w_L{}^2 [M]\{\phi\}_0 = [K_L]\{\phi\}_0 \quad (3.6.1)$$

where, $[M]$ and $[K_L]$ denote the system mass and linear stiffness matrices respectively, ϖ_L the fundamental linear frequency and $\{\phi\}_0$ the corresponding linear mode shape normalized with the maximum component to unity. The plate deflection $w_{\max}\{\phi\}_0$ is then used to obtain the non-linear stiffness matrix $[K_{NL}]$. The equation of motion for non-linear free vibration is written as

$$\varpi_{NL}{}^2 [M]\{\phi\}_I = ([K_L]+[K_{NL}])\{\phi\}_I \quad (3.6.2)$$

where, ϖ_{NL} is the fundamental non-linear frequency associated with the amplitude A ($= C/h$) and $\{\phi\}_I$, the corresponding normalized mode shape of the I^{th} iteration. The solution of equation (3.6.2) is obtained using the direct iteration method. The steps involved are:

***Step 1*:** The fundamental linear frequency and corresponding linear mode shape is calculated by solving equation (3.6.2) with all the terms in $[K_{NL}]$ being set to zero.

***Step 2*:** The mode shape is normalized by appropriately scaling the eigenvector ensuring that the maximum displacement is equal to the desired amplitude $W_{\max}/h$.

***Step 3*:** The terms in the stiffness matrix $[K_{NL}]$ are computed using the normalized mode shape.

Step 4: The equations are then solved to obtain new eigenvalues and corresponding eigenvectors.

***Step 5*:** Steps 2 to 4 are now repeated with $w_{\max}\{\phi\}_I$ until convergence criterion is satisfied.

The convergence criteria used in the present study are

(i) displacement norm defined as $\sum \Delta w_i^2 / \sum w_i^2$

and (ii) frequency norm defined as $|\Delta w_i| / w_i$

where, w_i and Δw_i are the change in displacement and change in non-linear frequency during the i^{th} iteration cycle.

Chapter - 4

COMPUTER PROGRAM

4.1 GENERAL

A computer program based on the formulation given in the previous chapter is developed in FORTRAN-77 for large amplitude vibration analysis of isotropic plates. The program is based on five degrees of freedom per node viz. u, v, w, θ_x *and* θ_y. Isotropic plates of rectangular as well as skew configurations have been analyzed by this program.

4.2 SALIENT FEATURES

The salient features of the computer program are given below:

a. Automatic mesh generation
b. Generation of linear element stiffness matrix and mass matrix generation
c. Generation of non-linear stiffness matrix
d. Generation of overall stiffness and mass matrices as a single array (skyline form)
e. Fitting of boundary conditions
f. Solution for dominant eigenvalues and eigenvectors by using Corr and Jennings simultaneous iteration method[4]
g. Optimum utilization of memory by removing zeros from matrices
h. Use of symmetry of the plate so as to reduce the CPU time

4.2.1 Automatic mesh generation

The mesh division for the structures analyzed is generated automatically. The algorithm for this purpose is provided in the main program itself. The plate structure is divided into a number of elements by assigning the number of divisions in each direction. This information is given as input to the problem under consideration. The elements are numbered automatically moving from left to right and top to bottom as shown in the Fig.4.1. Each element has eight nodes which are numbered consecutively from left hand top corner in a clockwise direction. For the whole structure, the nodes are numbered automatically, moving from left to right and from top to bottom.

Fig. 4.1 A TYPICAL MESH DIVISION

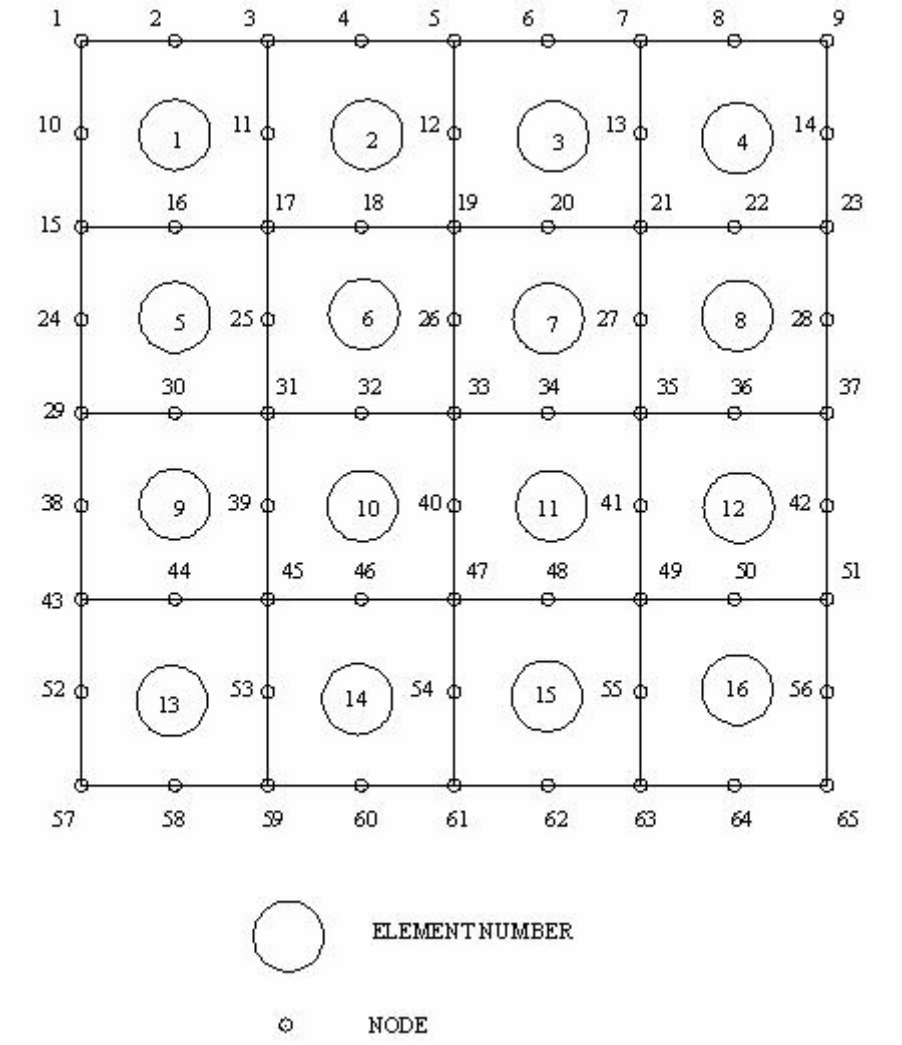

On the basis of the element dimensions, the coordinates of the eight nodes are calculated. If the elements are not of regular shape, then the coordinates of each node are to be indicated. The edges of the element are then mapped into straight edges through the use of shape functions. Based on the ξ, η values of the nodes, the x, y values of any point within the element can be obtained (Fig. 3.1) by the following relations:

$$x = \sum_{r=1}^{8} N_r \; X_r \qquad \text{and} \qquad y = \sum_{r=1}^{8} N_r \; Y_r \tag{4.2.1}$$

4.2.2 Linear element stiffness matrix

The element stiffness matrix for the plate is generated by the subroutine ELSM. The element stiffness matrix for the plate is generated and assembled in as a single array using skyline procedure. The material properties are read from main program. Subroutine ELSM generates $[B_L]$ needed for evaluation of the element stiffness matrix. The linear stiffness matrix of the element $[K_L]$ is given by

$$[K_L] = \int_{-1}^{1} [B_L]^T [D][B_L] |J| \, d\xi \, d\eta \tag{4.2.2}$$

The integration of the products of different matrices to obtain the element stiffness matrix is performed with the help of subroutine GACUV based on Gauss quadrature.

4.2.3 Non-linear element stiffness matrix

The non-linear element stiffness matrix $[K_{NL}]$ for the plate is generated by subroutine ELSMN. The expression for the non-linear element stiffness matrix is

$$[K_{NL}] = \frac{1}{2}[N_1] + \frac{1}{3}[N_2] \tag{4.2.3}$$

Various matrices involved in the above equation are generated by the subroutine ELSMN. The integration of the products is performed by GAUSS subroutine which is based on Gauss quadrature. The non-linear stiffness matrix is renewed iteratively as the element stiffness is formed using the latest value of displacement. Then the stiffness matrix is assembled and overall stiffness matrix is formed.

4.2.4 Overall stiffness matrix

The assembly of the stiffness matrices to obtain overall stiffness matrix as a single array (Fig. 4.2) based on skyline procedure is done by subroutine ASSEM. It first assembles plate element linear stiffness matrices and thereafter, it assembles non-linear stiffness matrices. The element stiffness matrices are then assembled to form overall stiffness matrix of the structure.

Fig. 4.2 TYPICAL DETAILS OF STORAGE OF STIFFNESS MATRIX

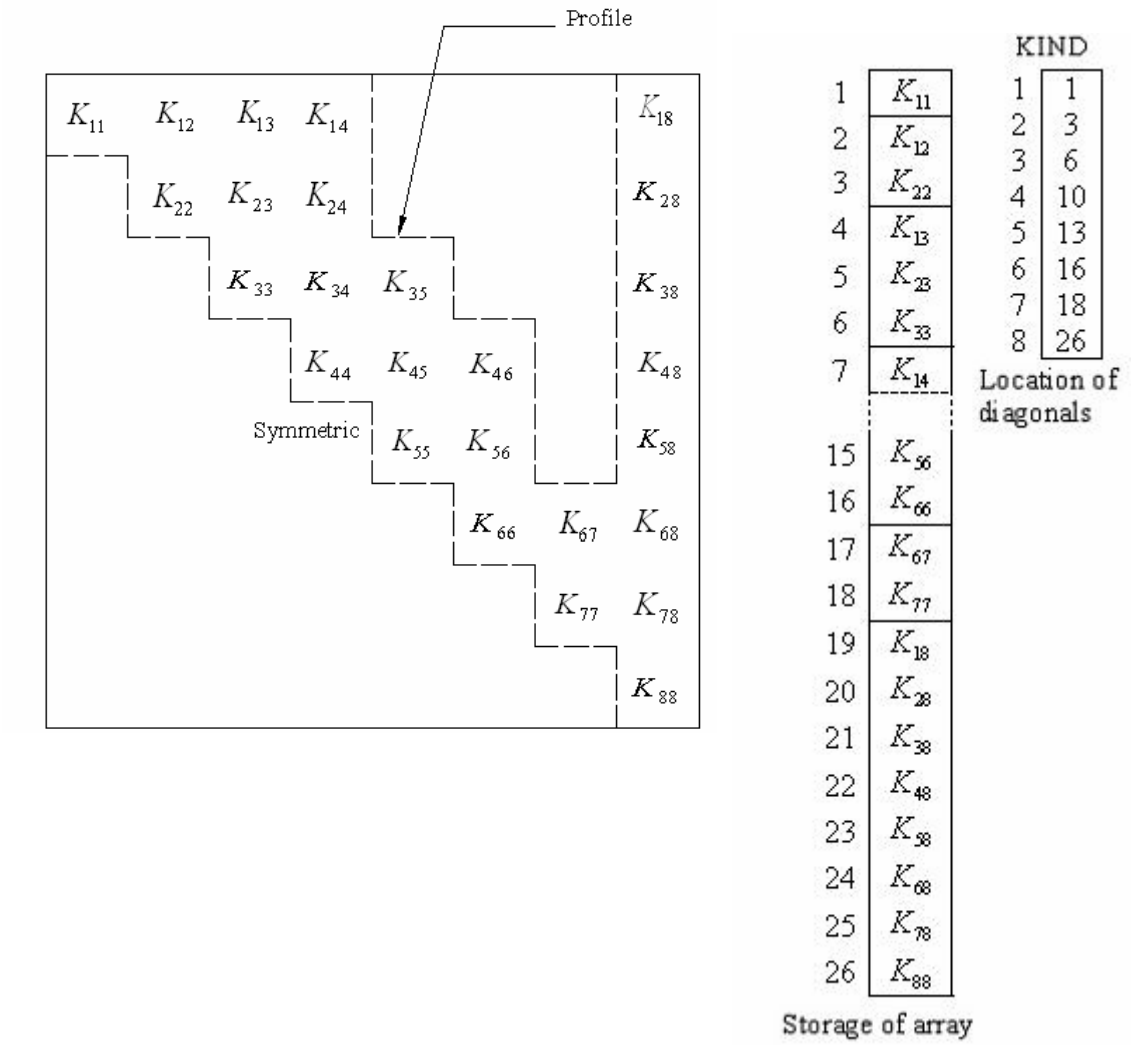

4.2.5 Fitting of boundary conditions

The support edges of the structure may be parallel to the global axes or may have some arbitrary orientation. If they are parallel, then all the displacements at the boundary can be satisfactorily taken into account. In such cases, the diagonal elements of the stiffness matrix corresponding to the restrained displacement levels at the boundary nodes are assigned very high numerical values, say 10^{20}. The shear force or the reaction at a node on a supported edge gives highly inaccurate values if the boundary conditions are not exactly satisfied. This happens in particular for skew plates where the support lines are not parallel to the global axes. In such cases, it is impossible to satisfy the boundary conditions if the overall stiffness matrix is formed in terms of the displacements corresponding to the global axes. In order to treat the inclined boundary conditions as normal constraints, the nodal displacements of these boundary nodes are transferred from the global axes to the coordinate system with one of the

axes tangent to the boundary node under consideration. This transformation is a simple point transformation involving direction cosines relating the global axes to the local axes system at the boundary. After obtaining the displacements of the boundary nodes in the transformed axes, the diagonal elements of the stiffness matrix corresponding to the displacement levels where restraints exist are assigned large numerical values.

4.2.6 Input data

The input data required for the analysis are as follows:

i. Plate dimensions,
ii. Mesh division, number of nodes of element, degrees of freedom at each node, number of Gauss points, number of loading conditions, degree of freedom of the amplitude taken as reference for normalizing,
iii. Boundary conditions of the structure,
iv. Material properties of the plate,
v. Number of amplitude levels and tolerance for convergence, and
vi. Amplitude data.

4.2.7 Output data

i. The input data,
ii. Linear frequency,
iii. Non-linear frequency, mode-shape error, frequency error and mode-shapes in each iteration, and number of iterations taken for convergence, and
iv. Number of iterations taken by the eigenvalue routine.

4.2.8 Program Flow

The program flow is hereby presented through the flow diagrams (Fig. 4.3-4.6). The entire program is controlled by a main program and several subroutines.

Fig. 4.3 Flow diagrams for MAIN & ALOKET

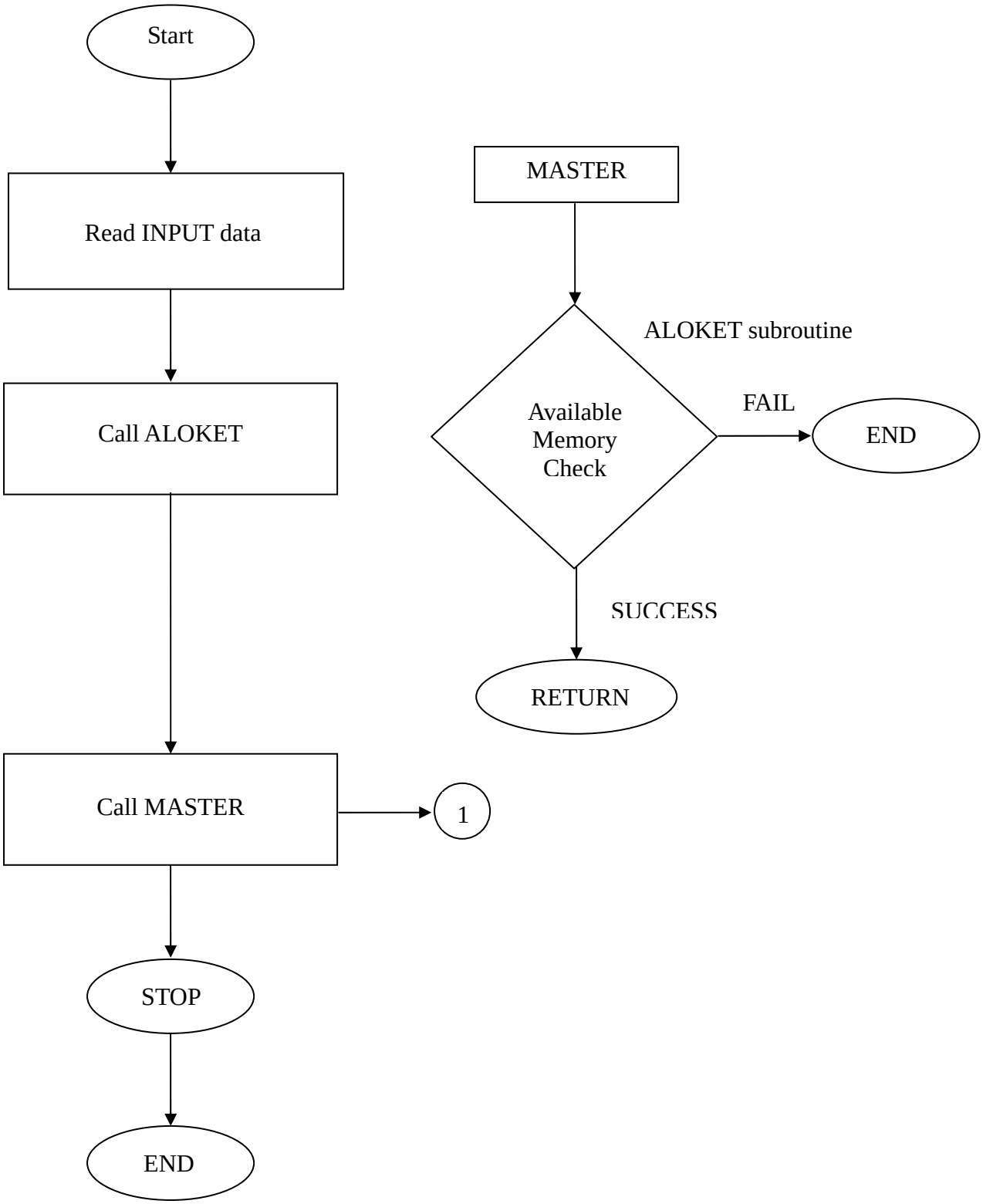

Fig. 4.4 Flow diagram for MASTER

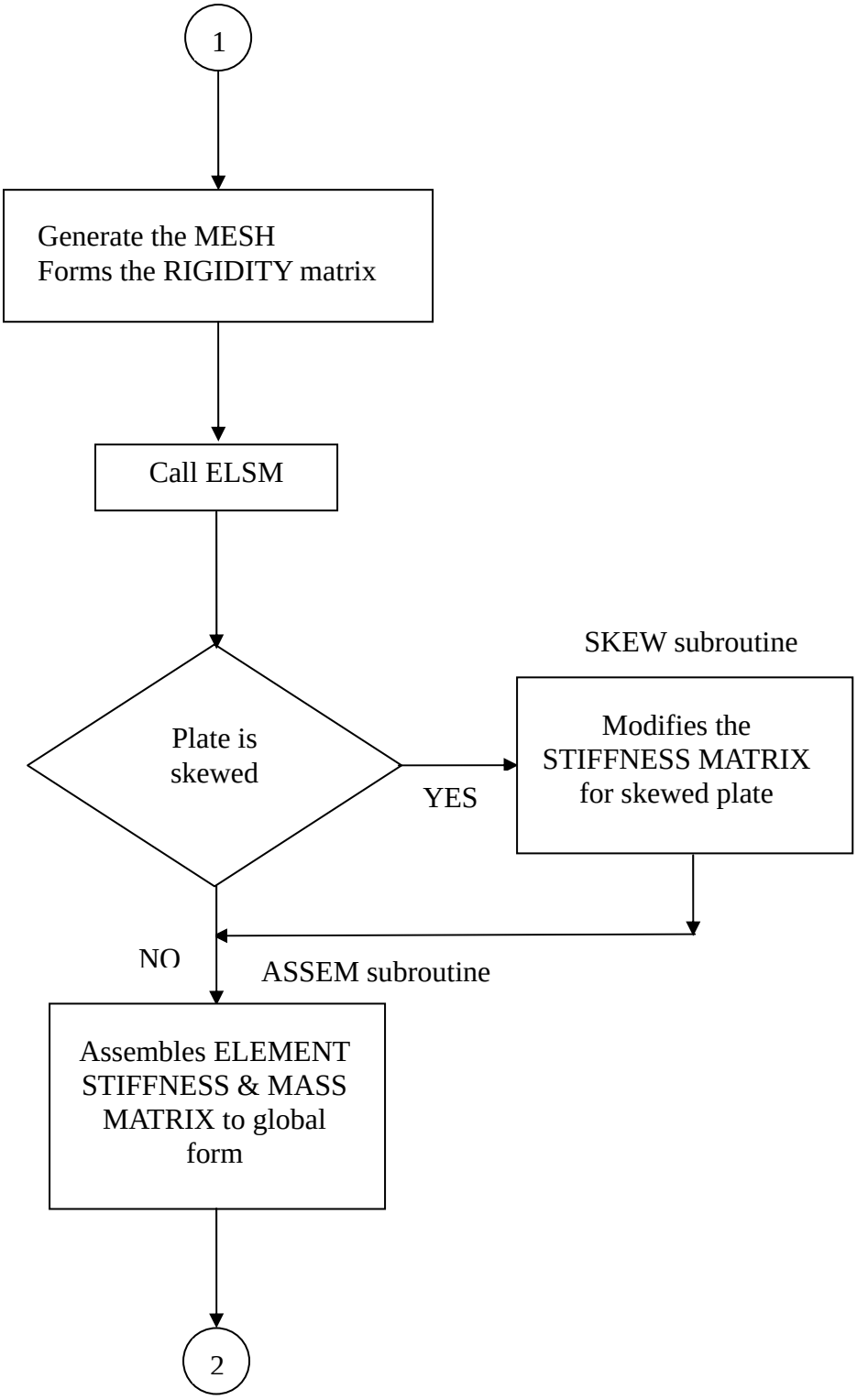

Fig. 4.5 Flow diagrams for ELSM & MASTER Contd…

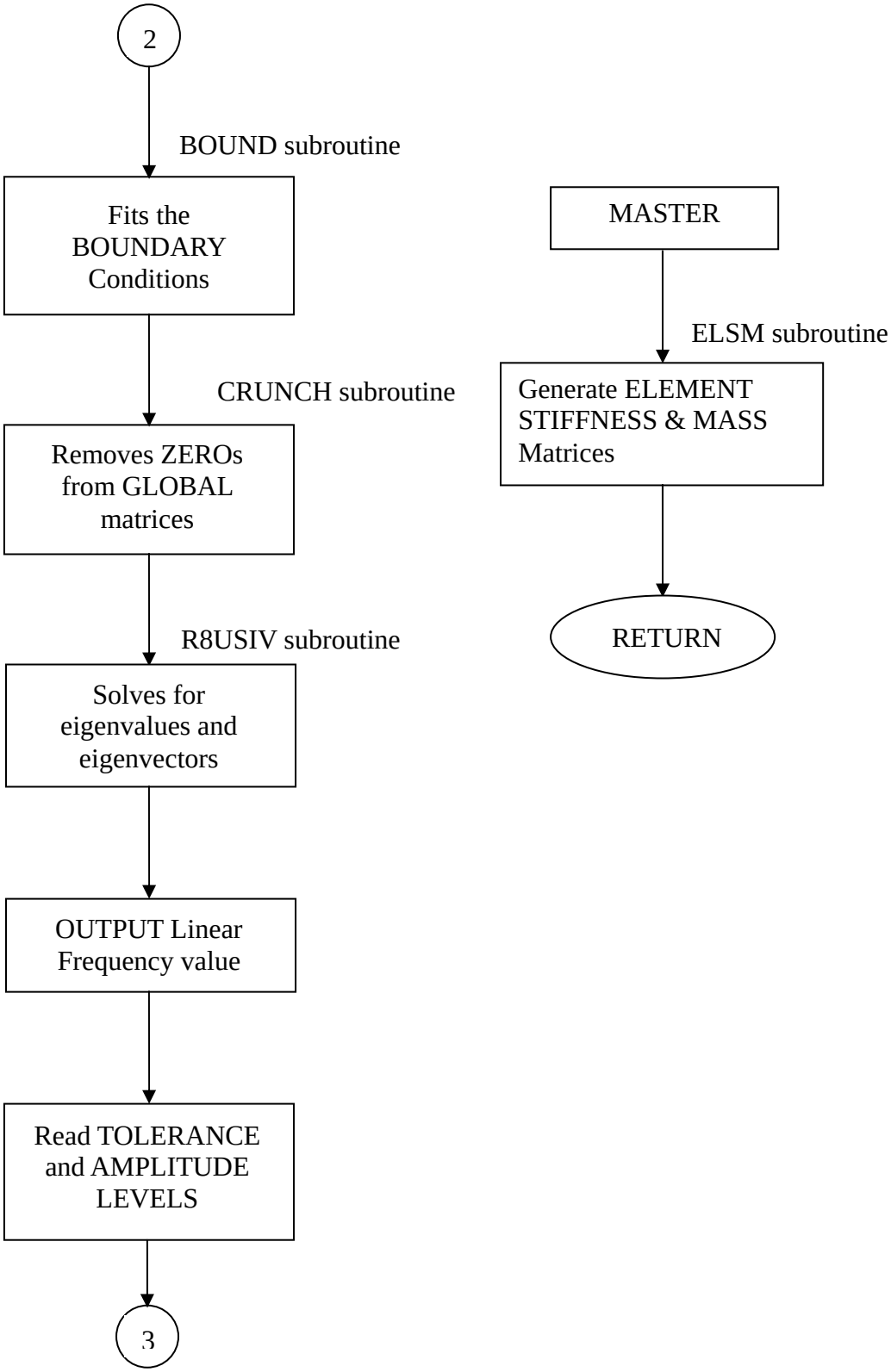

Fig. 4.6 Flow diagram for MASTER Contd…

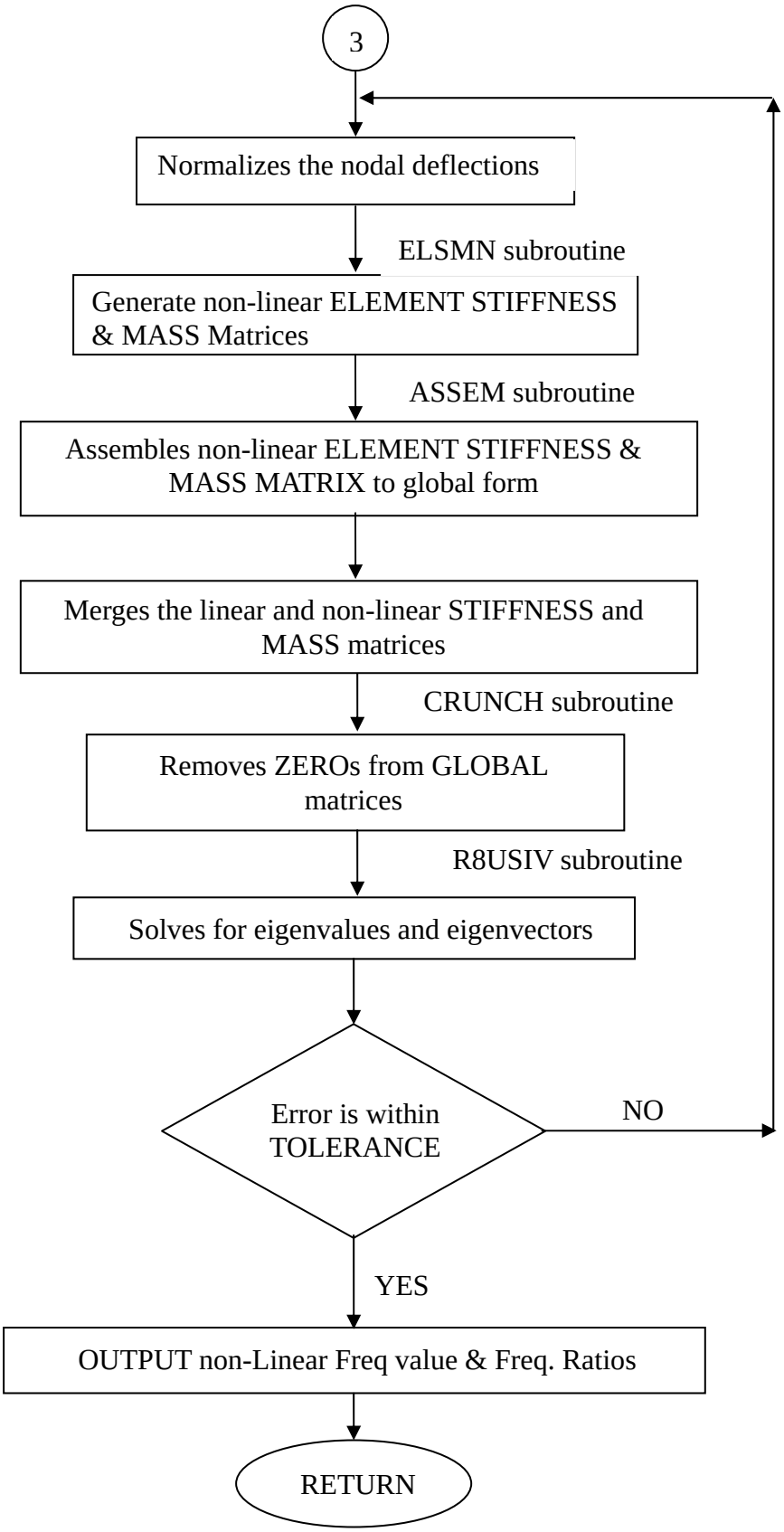

Chapter - 5

RESULTS & DISCUSSION

5.1 INTRODUCTION

The finite element formulation of large amplitude vibrations of isotropic plates has been presented in Chapter 3. The computer programming based on this method has been put forward in Chapter 4. Examples have been worked out to validate the proposed approach. A number of examples have been presented and comparisons have been made with the results of the earlier investigators wherever possible. The examples include square, rectangular and skew plates with various boundary conditions. All the problems have been solved by using the iterative technique presented by Corr and Jennings[4]. Unless and otherwise mentioned all problems have been solved using a mesh size of 6×6 for quarter of a plate.

5.2 EXAMPLES

5.2.1 SSSS square plate

Table 5.1 presents the non-linear frequency ratios (ϖ_{NL}/ϖ_{L}) of a simply supported square plate (Fig. 5.1) for the fundamental mode with amplitude to thickness ratios $\left(C/h\right)$ varying from 0.2 to 1.0. The results compare well with those of Goswami et al.[7], Ganapathy et al[6] & Rao et al[14].

Table 5.1 Non-linear Frequency ratios (ϖ_{NL}/ϖ_{L}) for square plate (SSSS)

	C/h				
	0.2	**0.4**	**0.6**	**0.8**	**1.0**
Present	1.0268	1.0995	1.2116	1.3545	1.5249
Goswami et al.	1.0263	1.1012	1.2165	1.3629	1.5325
Ganapathy et al.	1.02504	1.10021	1.20803	1.35074	1.51347
Rao et al.	1.0261	1.1009	1.2162	1.3624	1.5314

5.2.2 Square plate with various boundary conditions (CCCC, SSCC and SCSC)

Table 5.2 presents the non-linear frequency ratios for the fundamental mode for CCCC, SSCC, SCSC boundary conditions for a square plate for amplitude ratio $\left(C/h\right)$ values ranging from 0.2 to 1.0. The results have been compared with those of Rao et al.[13],

Mei[10] and Yamaki[21]. It can be seen that the values of the references are on the lower side. This is because of the different techniques chosen by them for the solution of the nonlinear equations. Their formulations have been based on appropriate linearization of the non-linear strain-displacement relations. They have also neglected the in-plane deformation terms. In the present investigation, the in-plane deformation terms have been considered and no approximating procedure is used. Hence the present results may be deemed as more accurate.

Table 5.2 Non-linear Frequency ratios (ϖ_{NL}/ϖ_{L}) for square plate with various boundary conditions

	C/h					**Boundary conditions**
	0.2	**0.4**	**0.6**	**0.8**	**1.0**	
Present	1.0098	1.0370	1.0812	1.1386	1.2099	**CCCC**
Rao et al.	1.007	1.0276	1.0608	1.1047	1.1578	
Mei	1.0062	1.0256	1.0564	1.0969	1.1429	
Yamaki	1.0085	1.0292	1.0661	1.1136	1.1674	
Present	1.0183	1.0689	1.1480	1.2473	1.3608	**SSCC**
Rao et al.	1.0139	1.0541	1.1169	1.1977	1.2918	
Mei	1.0138	1.0527	1.1119	1.1855	1.2705	
Present	1.0137	1.0518	1.1135	1.1928	1.2896	**SCSC**
Rao et al.	1.0097	1.0381	1.0838	1.1443	1.2174	
Mei	1.0097	1.0380	1.0833	1.1429	1.2143	

Fig. 5.1 Geometric & material properties of the square plate

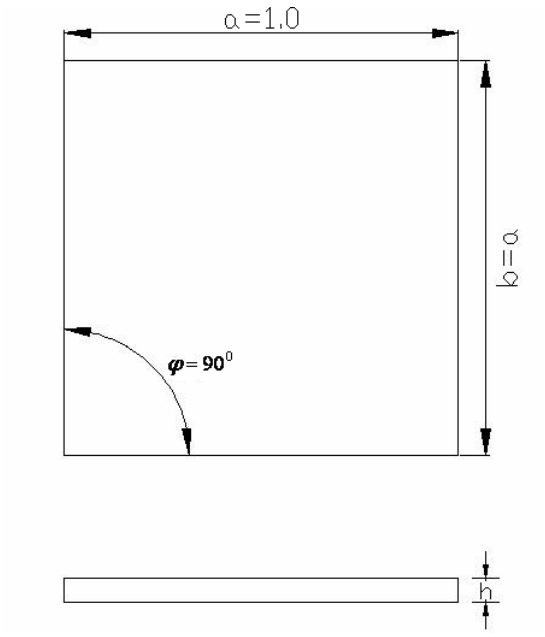

$$E = 10.92 \times 10^{6}\ N/m^{2}$$
$$h = 0.01\,m$$
$$\rho = 100.0\ kg/m^{3}$$
$$\upsilon = 0.3$$

5.2.3 CCCC rectangular plate

Table 5.3 presents the non-linear frequency ratios for the fundamental mode of CCCC rectangular plate with plate aspect ratio $\left(a/b\right)$ of 2.0 for the amplitude ratios $\left(C/h\right)$ ranging from 0.2 to 1.0. The results are in close agreement with that of Rao et al. [13].

Table 5.3 Non-linear Frequency ratios $\left(\varpi_{NL}/\varpi_{L}\right)$ for CCCC rectangular plate with aspect ratio $\left(a/b=2\right)$

	C/h				
	0.2	**0.4**	**0.6**	**0.8**	**1.0**
Present	1.0099	1.0393	1.0871	1.1505	1.2286
Rao et al.	1.0074	1.0292	1.0647	1.1123	1.1686

5.2.4 CCSS rectangular plate

Table 5.4 presents the comparison of non-dimensional frequency parameter results $\left(\lambda\right)$ of a CCSS rectangular plate, corresponding to various plate aspect ratios $\left(a/b\right)$ with that of Bikri et al. [2]. The values are found to be very close.

Table 5.4 Non-dimensional frequency parameter $\left(\lambda\right)$ for CCSS rectangular plate

	a/b				
	0.333	**0.4**	**0.5**	**0.667**	**1.0**
Present	16.42	16.91	17.81	20.00	27.08
Bikri et al.	16.38	16.85	17.77	19.96	27.06

5.2.5 Period ratio $\left(T_{NL}/T_{L}\right)$ for CCCC square and rectangular plates

Table 5.5 and Table 5.6 contain the non-linear period ratios $\left(T_{NL}/T_{L}\right)$ of a clamped-clamped square and a clamped-clamped rectangular plate $\left(a/b=2\right)$ respectively for the fundamental mode for amplitude ratios $\left(C/h\right)$ ranging from 0.2 to 1.0. The plates have been analyzed for a mesh size of 4×4. The results are close to those of Rao et al. [13].

Table 5.5 Non-linear Period ratios (T_{NL}/T_L) for a square plate (CCCC) for the fundamental mode

	C/h				
	0.2	**0.4**	**0.6**	**0.8**	**1.0**
Present	0.99197	0.97475	0.94554	0.90884	0.86725
Rao et al.	0.993	0.973	0.9424	0.9045	0.8624

Table 5.6 Non-linear Period ratios (T_{NL}/T_L) for a rectangular plate (CCCC) for the fundamental mode

	C/h				
	0.2	**0.4**	**0.6**	**0.8**	**1.0**
Present	0.99138	0.9668	0.92877	0.88135	0.83049
Rao et al.	0.9927	0.9717	0.9400	0.9011	0.8601

5.2.6 Effect of Poisson's ratio (υ)

Fig. 5.2 and Fig. 5.3 depict the effect of Poisson's ratio (υ) on the non-linear frequency ratio (ϖ_{NL}/ϖ_L) for a square plate with SSSS and CCCC boundary conditions respectively. From the graphs it can be seen that there is an increase in the frequency ratio with an increase of the Poisson's ratio at each amplitude levels. For a single material (*i. e.* constant Poisson's ratio) the higher the amplitude level the higher is the frequency ratio.

Fig. 5.2 Variation of non-linear Frequency ratio (ϖ_{NL}/ϖ_L) with Poisson's ratio of a square plate (SSSS) for the fundamental mode

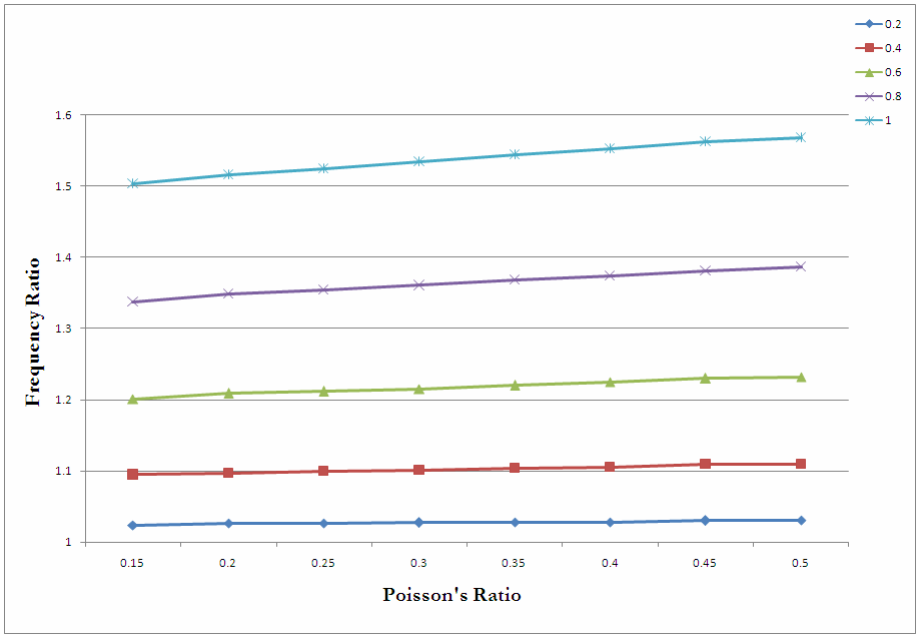

Fig. 5.3 Variation of non-linear Frequency ratio (ϖ_{NL}/ϖ_L) with Poisson's ratio of a square plate (CCCC) for the fundamental mode

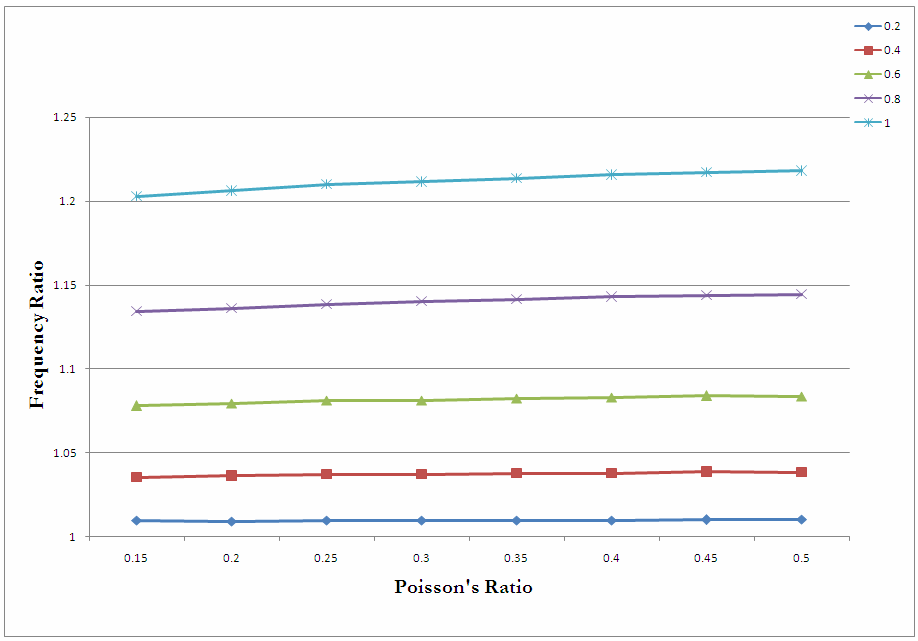

5.2.7 Effect of thickness parameter (a/h)

Fig. 5.4 and Fig. 5.5 show the variation of non-linear frequency ratio (ϖ_{NL}/ϖ_L) due to a change in the thickness parameter (a/h) for square plates with different boundaries. Fig. 5.4 is for a square plate simply supported on all sides. Fig. 5.5 gives the variation for the plate when it is clamped on all edges. It can be seen from all the graphs that the non-linear frequency ratio (ϖ_{NL}/ϖ_L) remains almost constant despite a change in the thickness parameter (a/h) .

5.2.8 Effect of aspect ratio (a/b)

Fig. 5.6 shows the variation of the non-linear frequency ratio (ϖ_{NL}/ϖ_L) for simply supported rectangular plates of different aspect ratios (a/b). It may be observed that there is an increase of the frequency ratio with the increase of the aspect ratio for the plates at all the amplitude levels.

Fig. 5.4 Variation of non-linear Frequency ratio $\left(\varpi_{NL}/\varpi_{L}\right)$ with thickness parameter $\left(a/h\right)$ of a square plate (SSSS) for the fundamental mode

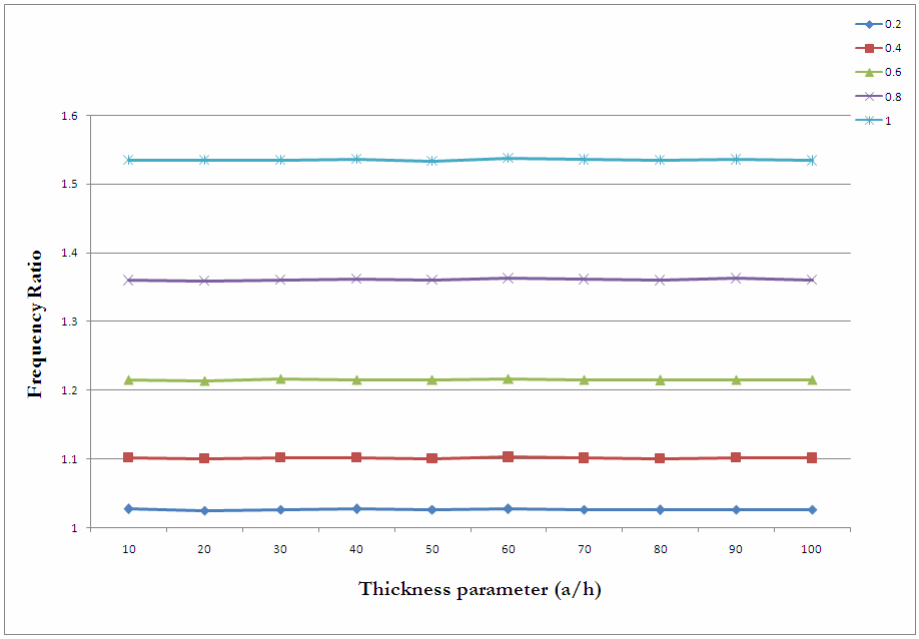

Fig. 5.5 Variation of non-linear Frequency ratio $\left(\varpi_{NL}/\varpi_{L}\right)$ with thickness parameter $\left(a/h\right)$ of a square plate (CCCC) for the fundamental mode

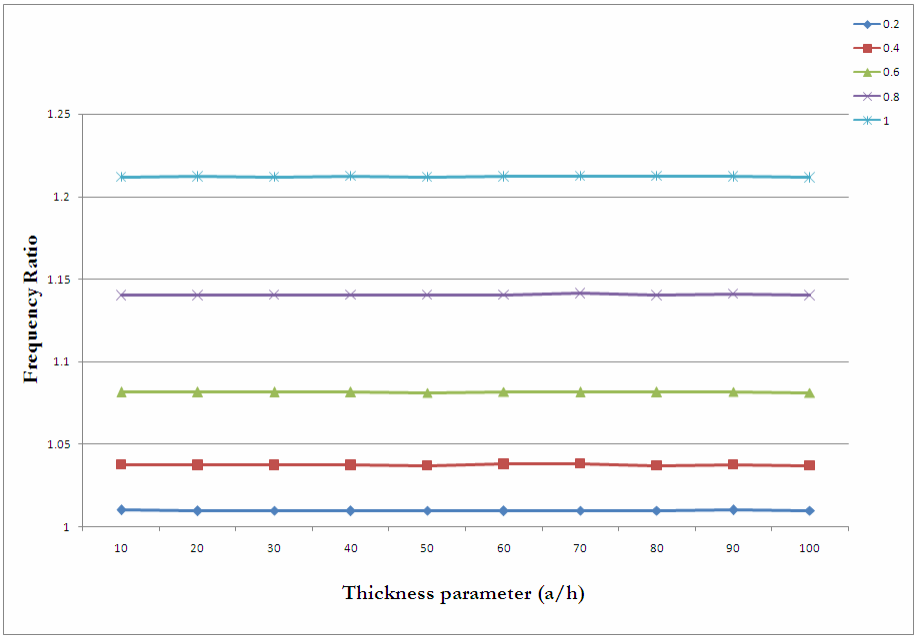

Fig. 5.6 Variation of non-linear Frequency ratio (ϖ_{NL}/ϖ_L) with aspect ratio (a/b) of a plate (SSSS) for the fundamental mode

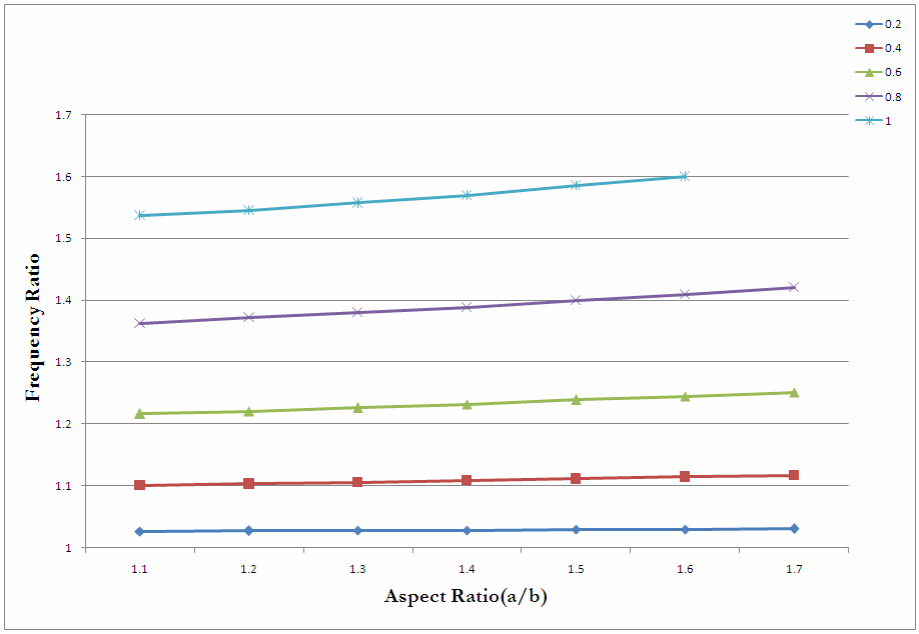

5.2.9 Effect of skew angle (φ)

Fig. 5.7 and Fig. 5.8 respectively denote the variation of the non-linear frequency ratio (ϖ_{NL}/ϖ_L) with the skew angle (φ) of the square plate for SSSS and CCCC support conditions. For SSSS boundary it is observed that for any amplitude level the frequency ratio first decreases and then again increases as the skewness of the plate is decreased. But for a CCCC boundary it is observed that the decrease in skewness reduces the frequency ratio at all the amplitude levels.

Table 5.7 lists the results for non-dimensional fundamental frequency parameter (λ) for a rhombic plate with all edges simply supported. The obtained results have been compared with Das et al. [5] and found to be well matching. Table 5.8 gives the value of λ for a rhombic plate under different boundary conditions. Table 5.9 contains the values of the dimensionless fundamental frequency parameter for a skew plate with plate aspect ratio of 2.0 under different support conditions.

Table 5.7 Non dimensional frequency parameter (λ) for a rhombic plate (SSSS) for the fundamental mode

	$\phi(^\circ)$			
	15	**30**	**45**	**60**
Present	20.832	25.4022	37.1037	71.9729

Das et al.	20.889	25.065	35.680	66.84

Table 5.8 Non dimensional frequency parameter (λ) for a rhombic plate for the fundamental mode for different boundary conditions (CCCC, SCSC, SSCC)

Boundary Conditions	$\phi(^\circ)$			
	15	**30**	**45**	**60**
CCCC	38.6211	46.6082	65.8015	117.6328
SCSC	30.7205	36.8956	51.4998	90.325
SSCC	21.6176	34.1922	47.8603	86.1482

Table 5.9 Non dimensional frequency parameter (λ) for a skew plate with aspect ratio 2 for the fundamental mode for different boundary conditions (SSSS, CCCC, SCSC, SSCC)

Boundary Conditions	$\phi(^\circ)$			
	15	**30**	**45**	**60**
SSSS	52.2715	63.919	93.3185	178.3627
CCCC	105.1056	128.8644	188.8347	365.7246
SCSC	58.016	69.62	98.5784	182.4063
SSCC	75.5159	92.0309	133.9075	257.7675

Fig. 5.7 Variation of non-linear Frequency ratio (ϖ_{NL}/ϖ_L) with skew angle (φ) of a square plate (SSSS) for the fundamental mode

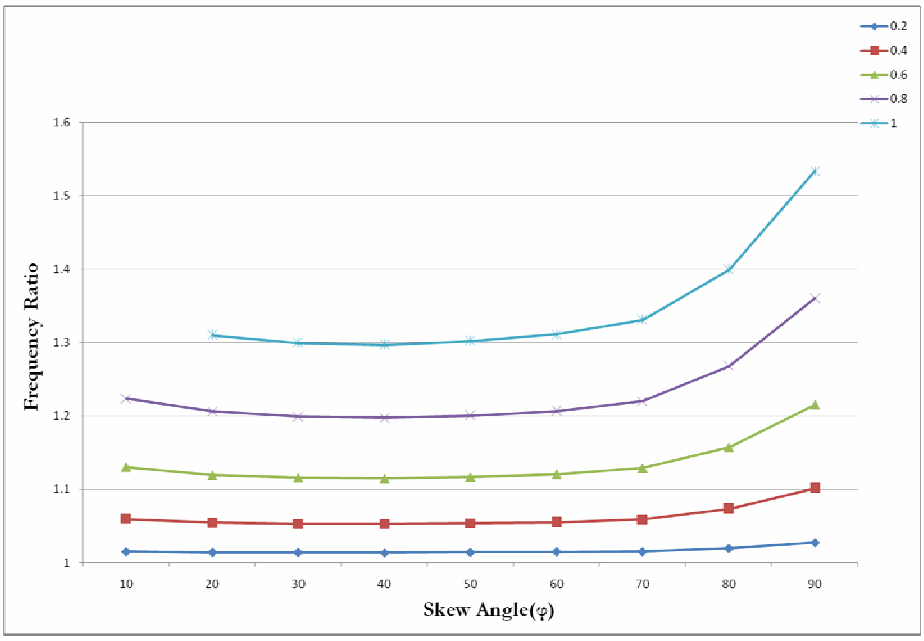

Fig. 5.8 Variation of non-linear Frequency ratio $\left(\varpi_{NL}/\varpi_{L}\right)$ with skew angle (φ) of a square plate (CCCC) for the fundamental mode

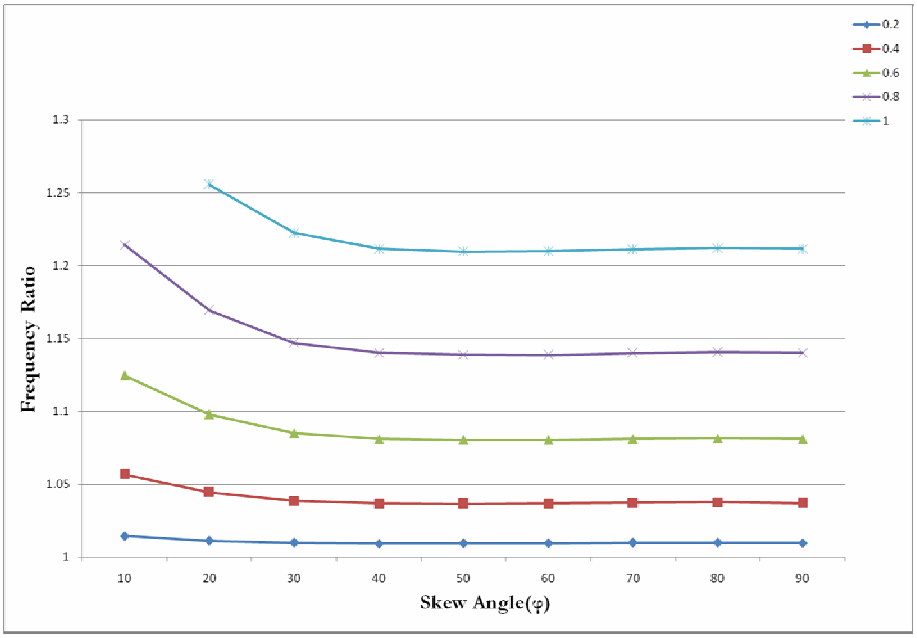

Chapter - 6

CONCLUSIONS

CONCLUSIONS

The following conclusions may be made from the present investigation of the large amplitude free vibration analysis for rectangular and skew plates:

1. The boundary conditions of the plate directly affect the degree of the non-linearity assessed through the non-linear frequency ratio. More restrained boundaries tend to produce lower values of non-linear frequency.

2. For the materials having higher Poisson's ratio, the non-linear frequency have been observed to be higher.

3. At lower values of vibration amplitudes the Poisson's ratio has no significant effect on the non-linear frequency of vibration. But as the amplitudes of vibration increase there is remarkable increase in the non-linear frequency ratio.

4. There is no significant effect on the non-linear frequency ratio with the change in the thickness parameter.

5. The non-linear frequency ratio varies directly with respect to the plate aspect ratio. The increase in the aspect ratio shifts the non-linear frequency towards the higher side.

6. For a simply supported square plate the non-linear frequency ratio first decreases slightly and then increases as the angle of skewness is increased.

7. For a clamped-clamped square plate the non-linear frequency ratio increases as the angle of skewness is increased.

REFERENCES

REFERENCES

[1] Bathe K. J. “Finite Element Procedures”, New Delhi: *Prentice-Hall of India, **(1996)***

[2] Bikri K. El, Benamar R. & Bennouna M., “Geometrically Non-Linear Free Vibrations of Clamped Simply Supported Rectangular Plates. Part I: The Effects of Large Vibration Amplitudes on the Fundamental Mode Shape.” *Computers and Structures,* 81, ***(2003): p. 2029–2043***

[3] Benamar R., Bennouna M. K. K. & White R. G., “The Effects of Large Vibrations Amplitudes On The Fundamental Mode Shape of A Fully Clamped, Symmetrically Laminated Rectangular Plate.”, *Fourth International Conference of Recent advances in Structures Dynamics, (**1990): p. 749–60***

[4] Corr R. B. & Jennings A., “A Simultaneous Iteration Algorithm for Symmetric Eigenvalue Problems.”, *International Journal for Numerical Methods in Engineering, 10, **(1976): p. 647-663***

[5] Das D., Sahoo P. & Saha K., “Large-amplitude Dynamic Analysis of Simply Supported Skew Plates by Variational Method.” *Journal of Sound and Vibration, 313, **(2008): p. 246-267***

[6] Ganapathy M., Vardhan T. K. & Sarma B. S., “Non-linear Flexural Vibrations of Laminated Orthotropic Plates.” *Computers and Structures, 39(6), **(1991): p. 685-688***

[7] Goswami Sanjib & Kant Tarun, “Large Amplitude Vibration of Polymer Composite Stiffened Laminates by Finite Element Method.” *Journal of Reinforced Plastics and Composites, 18, **(1999)**: **p. 421-436***

[8] Harras B., Benamar R. & White R. G., “Geometrically Non-linear Free Vibration of Fully Clamped Symmetrically Laminated Rectangular Composite Plates.” *Journal of Sound and Vibration, 251(4), **(2002): p. 579-619***

[9] Hinton E. & Owen D. R. J. “Finite Element Software for Plates and Shells”, Swansea, U.K.: *Pineridge Press Limited, **(1984)***

[10] Mei Chuh, “Large Amplitude Free Flexural Vibrations of Beams and Plates.” *Computers and Structures, 6, **(1976): p. 163-167***

[11] Mukhopadhyay M. & Seikh Abdul Hamid. “Matrix and Finite Element Analyses of Structures”, Delhi: *Gopal JeeEnterprises, **(2004)***

[12] Pandit M. K., Haldar S. & Mukhopadhyay M., “Free Vibration Analysis of Laminated Composite Rectangular Plate Using Finite Element Method.” *Journal of Reinforced Plastics and Composites, 26, **(2007): p. 69-80***

[13] Rao G.. Venkateswara, Raju I. S. & Raju K. Kanak, “A Finite Element Formulation for Large Amplitude Flexural Vibrations of Thin Rectangular Plates.” *Computers & Structures, 6, **(1976)**: **p. 163-167***

[14] Rao S. R. et al., “Large Amplitude Finite Element Vibration of Plates/Stiffened Plates”, *Journal of the Acoustical Society of America, 93(6), **(1993)**: **p. 3250-3257***

[15] Ray A. K., Banerjee B. & Bhattacharjee B., “Large Amplitude Free Vibrations of Skew Plates Including Transverse Shear Deformation and Rotatory Inertia- A new approach.” *Journal of Sound and Vibration, 180(4), **(1995): p. 669-681***

[16] Saha K. N., Mishra D., Ghosal S. & Pohit G., “Nonlinear Free Vibration Analysis of Square Plates With Various Boundary Conditions.” *Journal of Sound and Vibration, 287, **(2005): p. 1031-1044***

[17] Sarma M. S., Rao A. Venkateshwar, Pillai S. R. R. & Rao B. Nageswara, “Large Amplitude Vibrations of Laminated Hybrid Composite Plates.” *Journal of Sound and Vibration*, 159(3), ***(1992): p. 540-545***

[18] Sathyamoorthy M. & Pandalal K. A. V., “Large Amplitude Vibrations of Certain Deformable Bodies: Part II –plates and shells.” *Journal of Aeronautical Society of India 25,* ***(1973): p. 1-10***

[19] Sathyamoorthy M., “Non-linear Vibrations of Plates: A review.” *Shock and Vibration Digest, 15,* ***(1983b): p. 3-16***

[20] Sathyamoorthy M., “Non-linear Vibration of Analysis of Plates: A review and survey of current developments.” *Applied Mechanical Review, 40,* ***(1987): p. 1553-1561***

[21] Yamaki M., “Influence of Large Amplitudes on Flexural Vibrations of Elastic Plates.” *Journal of Applied Mathematics and Mechanics, 41,* ***(1961): p. 501-518***

[22] Zienkiewicz O. C. “The Finite Element Method”, New Delhi: *Tata McGraw-Hill Publishing Co. Ltd.* ***(1977)***